# DESIGN AND SYNTHESIS OF A BODIPY BASED PROBE FOR CADMIUM IONS

A Thesis Submitted to
the Graduate School of Engineering and Sciences of
İzmir Institute of Technology
in Partial Fulfillment of the Requirements for the Degree of

**MASTER OF SCIENCE**

in Chemistry

by
**Miray CEBECİ**

**December 2021**
**İZMİR**

# ACKNOWLEDGEMENTS

# ABSTRACT

## DESIGN AND SYNTHESIS OF A BODIPY BASED PROBE FOR CADMIUM IONS

Given the severely toxic effects of heavy metals on living systems and the environment in general, identifying and quantifying heavy metal ions in synthetic samples and in vivo are highly significant activities. One such heavy metal, cadmium, allows only a low level of tolerable exposure and can thus have fatal consequences or cause critical health problems such as ostial disorders, nephrotic syndromes, various types of cancer even in extremely low concentrations.

Although several standard techniques for detecting cadmium have been used, including atomic absorption and emission spectroscopy and inductively coupled plasma mass spectrometry, all of them require complex instruments that are also expensive, time-consuming to use, and hardly portable. For that reason, sensitive, selective, less labour-intensive methods of detecting cadmium ions are greatly needed. In response, fluorogenic or chromogenic methods afford high analyte sensitivity and selectivity, easy sample preparation, and easy monitoring, all with affordable instrumentation.

Against that background, this thesis reports the design, synthesis, and development of a fluorescent molecular sensor that can detect $Cd^{2+}$ ions within spectroscopic behavior and living cells. In the design, based on the mechanism of intramolecular charge transfer (ICT), borondipyrromethene (BODIPY) dye was used as a signal reporter due to its unique properties, and di-(2-picolyl)amine (DPA) was chosen to represent the recognition unit. Altogether, the sensor offers rapid response, high selectivity, and high sensitivity in detecting Cd ions is reversible with the aid of $CN^-$ and can be used to efficiently image $Cd^{2+}$ species in vitro.

# ÖZET

## KADMİYUM İYONLARI İÇİN BODIPY BAZLI ALGILAYICININ TASARIMI VE SENTEZİ

Ağır metallerin canlı sistemler ve genel olarak çevre üzerindeki ciddi toksik etkileri göz önüne alındığında, ağır metal iyonlarının sentetik numunelerde ve in vivo olarak tanımlanması ve ölçülmesi oldukça önemli faaliyetlerdir. Böyle bir ağır metal olan kadmiyum, yalnızca düşük düzeyde tolere edilebilir maruziyete izin verir ve bu nedenle ölümcül sonuçlara yol açabilir veya aşırı düşük konsantrasyonlarda bile ostial bozukluklar, nefrotik sendromlar, çeşitli kanser türleri gibi kritik sağlık sorunlarına neden olabilir.

Kadmiyumu saptamak için atomik absorpsiyon ve emisyon spektroskopisi ve indüksiyonla birleşmiş plazma kütle spektrometrisi dahil olmak üzere birkaç standart teknik kullanılmış olmasına rağmen, bunların tümü aynı zamanda pahalı, kullanımı zaman alıcı ve zor taşınabilir olan karmaşık aletler gerektirir. Bu nedenle, kadmiyum iyonlarını saptamak için hassas, seçici, daha az emek yoğun yöntemlere büyük ihtiyaç duyulmaktadır. Buna karşı, florojenik veya kromojenik yöntemler, tümü uygun fiyatlı enstrümantasyonla yüksek analit duyarlılığı ve seçiciliği, kolay numune hazırlama ve kolay izleme sağlar.

Bu bağlamda, bu tez, spektroskopik davranış ve canlı hücreler içindeki $Cd^{2+}$ iyonlarını tespit edebilen bir floresan moleküler sensörün tasarımını, sentezini ve gelişimini rapor eder. Molekül içi yük transferi (ICT) mekanizmasına dayanan tasarımda, benzersiz özelliklerinden dolayı sinyal algılayıcı olarak borondipirrometen (BODIPY) boyası kullanılmış ve di-(2-pikolil)amin (DPA) seçilmiştir. Toplamda, sensör hızlı tepki, yüksek seçicilik ve Cd iyonlarının tespitinde yüksek hassasiyet sunar ve $CN^{-}$ yardımıyla tersine çevrilebilir ve $Cd^{2+}$ türlerini in vitro olarak verimli bir şekilde görüntülemek için kullanılabilir.

# TABLE OF CONTENTS

# LIST OF FIGURES

# LIST OF ABBREVIATIONS

| | |
|---|---|
| **µL** | Microliter |
| **$\lambda_{abs}$** | Absorbance Wavelength |
| **$\lambda_{em}$** | Emission Wavelength |
| **$\lambda_{ex}$** | Excitation Wavelength |
| **Abs** | Absorbance |
| **ACN** | Acetonitrile |
| **ACN-$d_3$** | Deuterated Acetonitrile |
| **$BF_3. Et_2O$** | Boron Trifluoride Etherate |
| **BODIPY** | Boron Dipyrromethene |
| **DAPI** | 4′,6-diamidino-2-phenylindole |
| **DCM** | Dichloromethane |
| **DMF** | Dimethylformamide |
| **DMSO** | Dimethyl Sulfoxide |
| **DPA** | Di-(2-picolyl)amine |
| **Em.** | Emission |
| **Eq.** | Equivalent |
| **$Et_3N$** | Triethylamine |
| **EtOAc** | Ethyl Acetate |
| **EtOH** | Ethyl Alcohol |
| **Fig.** | Figure |
| **h** | Hour |
| **HEPES** | N-(2-Hydroxyethyl)piperazine-N′-(2-ethane sulfonic acid) |

| | |
|---|---|
| **HNO₃** | Nitric Acid |
| **H₂O** | Water |
| **HRMS** | High-Resolution Mass Spectroscopy |
| **HOMO** | Highest Occupied Molecular Orbital |
| **ICT** | Intramolecular Charge Transfer |
| **LUMO** | Lowest Unoccupied Molecular Orbital |
| **M** | Molar |
| **MeOH** | Methyl Alcohol |
| **Mg** | Milligram |
| **MgSO₄** | Magnesium Sulfate |
| **mix.** | Mixture |
| **mL** | Milliliter |
| **mmol** | Millimole |
| **NH₂NH₂.H₂O** | Hydrazine monohydrate |
| **nM** | NanoMolar |
| **NMRS** | Nuclear Magnetic Resonance Spectroscopy |
| **PBS** | Phosphate-Buffered Saline |
| **Pd/C** | Palladium on Carbon |
| **RT** | Room Temperature |
| **TLC** | Thin Layer Chromatography |
| **UV** | Ultraviolet |
| **v/v** | Volume to Volume Ratio |

# CHAPTER 1

# INTRODUCTION

## 1.1 An Overview

Discovered in 1817 in Germany by Friedrich Stromeyer, cadmium is a soft, ductile, silvery heavy transition metal with the symbol Cd and atomic number 48. Although cadmium was first used as dye pigments in its sulphide forms and in dental amalgams in the years after its discovery, it served as a substitute for tin during World War II and has more recently become widely used in industry and agriculture, including in nickel–cadmium batteries, pigment production, electroplating for metals, special alloys, metallurgical works, stabilizers for plastics, and even phosphate fertilizers (Pakalin et al., 2008; Tran and Popova, 2013). However, the U.S. Environmental Protection Agency lists cadmium as one of 126 priority pollutants owing to its non-biodegradability and long elimination half-life (i.e. 10–30 years).

Cadmium is indeed a highly toxic element that is easily absorbed and accumulated by plants and other organisms, causes water, soil, food pollution when overused, and consequently increases the risk of human exposure. Because cadmium is detrimental to all living things, it is responsible for critical environmental problems such as the prevention of plant growth, the decolouration of leaves, reduced yields in plant production, and health problems for humans, including renal disease, ostial disorders, anosmia, reproductive diseases in males, and various types of cancer. Beyond that, mounting evidence suggests that cadmium is a probable aetiological factor of neurodegenerative diseases such as Parkinson's and Alzheimer's disease (Zhang and Reynolds, 2019; Dukic-Cosic et al., 2020).

All of those traits of cadmium urge the development of methods of detecting and monitoring cadmium levels in vitro and in vivo for various areas of research. Although, several analytical techniques have been proposed for the detecting $Cd^{2+}$ -including voltammetry, atomic absorption spectroscopy (AAS), and inductively coupled plasma mass spectroscopy (ICP-MS), those techniques have several

limitations—for instance, expensive instrumentation, time-consuming procedures, demanding sample pre-treatment, and a lack of suitability for real-time monitoring. By contrast, fluorescent sensors are a preferable alternative due to their simplicity, rapid response, low detection limit, cost-effectiveness, high selectivity, and high sensitivity.

## 1.2. Fluorescent Sensors

Used in areas such as the natural sciences, technology, medicine, and engineering, sensors represent a class of devices able to detect environmental changes and events in light, gas, motion, pressure, humidity, and heat and give readable information about them. Chemosensors in particular are fluorescent-based sensors that detect specific chemical species and generate measurable responses. Every chemosensor contains two or three basic components: a fluorophore unit, a receptor unit, and/or a spacer or linker. Whereas a fluorophore unit emits the light that it absorbs, the receptor unit recognizes the target analyte or analytes, while a spacer links the fluorophore and receptor to each other. Many organic dyes are used as fluorophore units, including rhodamine, fluorescein, coumarin, and derivatives of 4,4-difluoro-4-bora-3a,4a-diaza-s-indacene—that is, boron dipyrromethene (BODIPY).
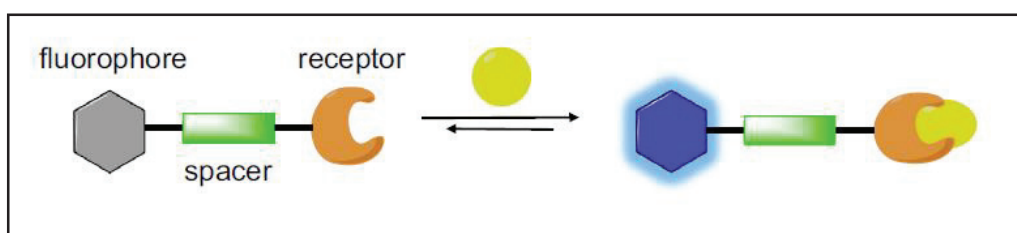


Figure 1.1. Schematic representation of design concept for the fully-construction fluorescent chemosensors (Source: Guo et al., 2021)

## 1.2.1. BODIPY as a Fluorophore

BODIPY, is a class of dyes first reported by Treibs and Kreuzer in 1968 (Treibs and Kreuzer, 1968). When they attempted tried to synthesize acetylated dimethylpyrrole, they led to achieved the acylation of 2,4-dimethylpyrrole with acetic anhydride and boron trifluoride as a potent fluorescent compound (Figure 1.2.).
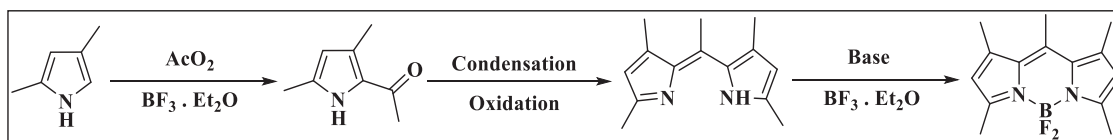
Figure 1.2. The first synthesis of BODIPY (Source: Treibs and Kreuzer, 1968)

Although the description of BODIPY for the IUPAC numbering system differs from that of dipyrromethene, they have the same α-, β-, and meso-positions for their carbon atoms. The meso- position is used for the central carbon, while the C atom next to N is named as the α-carbon, and other C atoms are indicated as β-carbons. Each C atom on the molecule is highly reactive and, thus facilitates modification to obtain the desired properties Figure 1.3.).
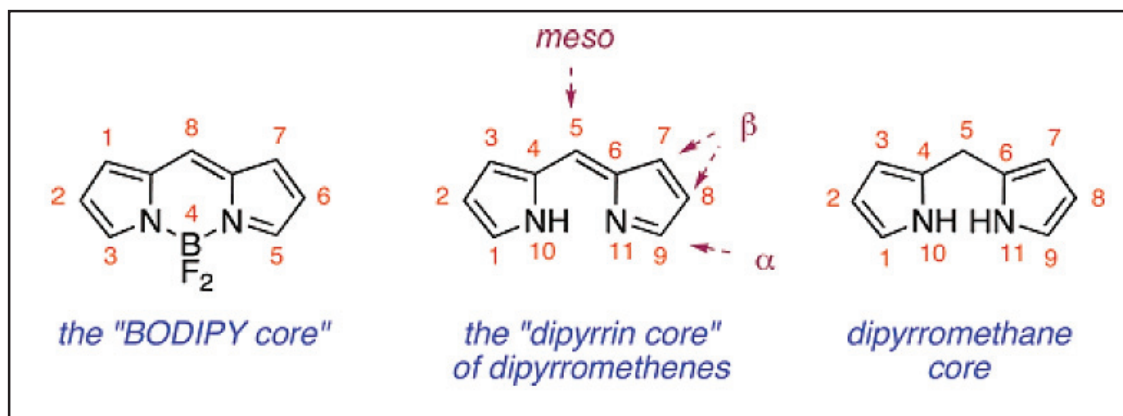


Figure 1.3. IUPAC numbering system of a boron dipyrrin compound

(Source: Loudet and Burgess, 2007)

BODIPY dyes are good fluorophores for designing highly sensitive, highly and selective sensors for cadmium ions given their narrow absorption and emission peaks, high fluorescence quantum yield, good chemical stability, general insensitivity to the pH of its medium, robust chemical properties, and ability to be readily functionalised to all possible positions of its core, which has maximum absorption and emission wavelengths between 480 and 540 nm. (Tao et al., 2019; Boens et al., 2019).

Because BODIPY dyes can be easily modified, chemical alteration can be applied to readily alter the spectroscopic properties. Those changes—for instance, derivatisation of α-, β- and meso positions of the BODIPY core and, the enlargement or shortening of the π-conjugation—affect the photophysical and spectroscopic properties of the fluorophore like absorbance and emission maxima or quantum yields. For instance,

because alkyl groups are added to the backbone of BODIPY, no significant change is observed in spectroscopic measurements. However, introducing a phenyl group to the meso-position influences its quantum yield because the rotation of the phenyl quenches its fluorescent events. Conjugation is another of BODIPY's important parameters. If the conjugation of BODIPY is switched, then blue or redshifts can be observed on the absorption and emission spectra.
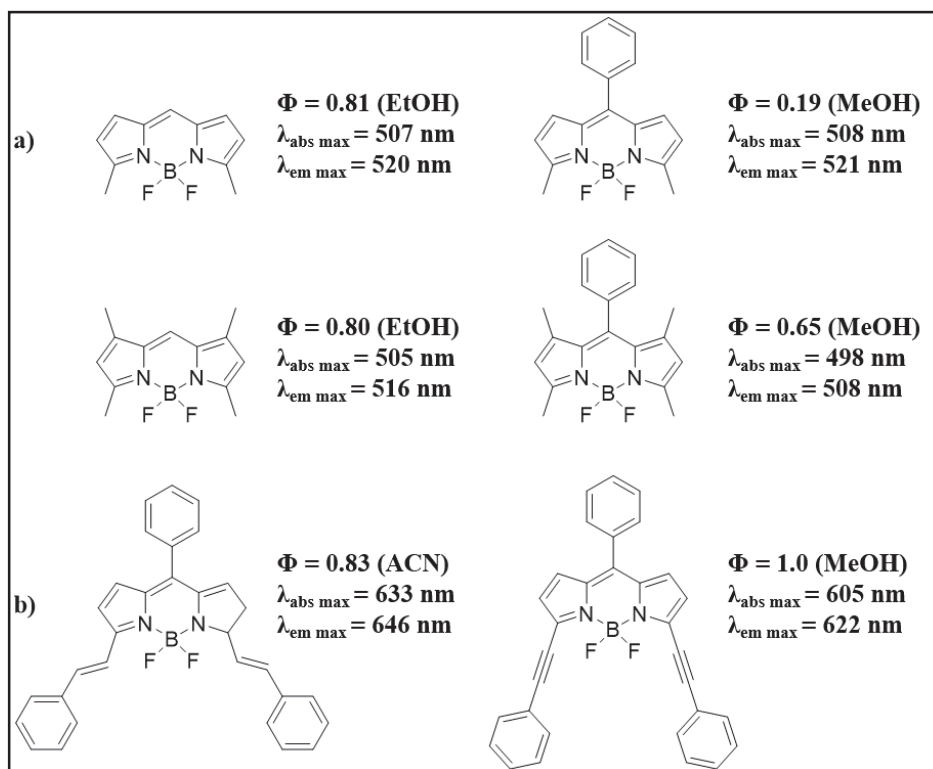


Figure 1.4. a) Influence of alkyl and meso aryl substituents on the spectroscopic properties of BODIPY (Source: Loudet and Burgess, 2007) b) Influence of extension conjugation of BODIPY structure (Source: Ni and Wu, 2014)

Beyond that, BODIPY fluorophores have remarkable chemical and photophysical features that had nevertheless received hardly any attention from researchers until 30 years ago. Monsma and colleagues first reported labeling proteins for biological applications using BODIPY (Monsma et al., 1989). Since then, BODIPY has enjoyed wide application, including in fluorescent markers for bio-imaging (Kowada et al., 2015), in photodynamic therapy agents (Turksoy et al., 2017), in laser dyes (Ortiz et al., 2010), and in fluorescent probes for gases (Cao et al., 2019), for pH (Teknikel and Unaleroglu, 2015), and for metal sensing (Carter et al., 2014).
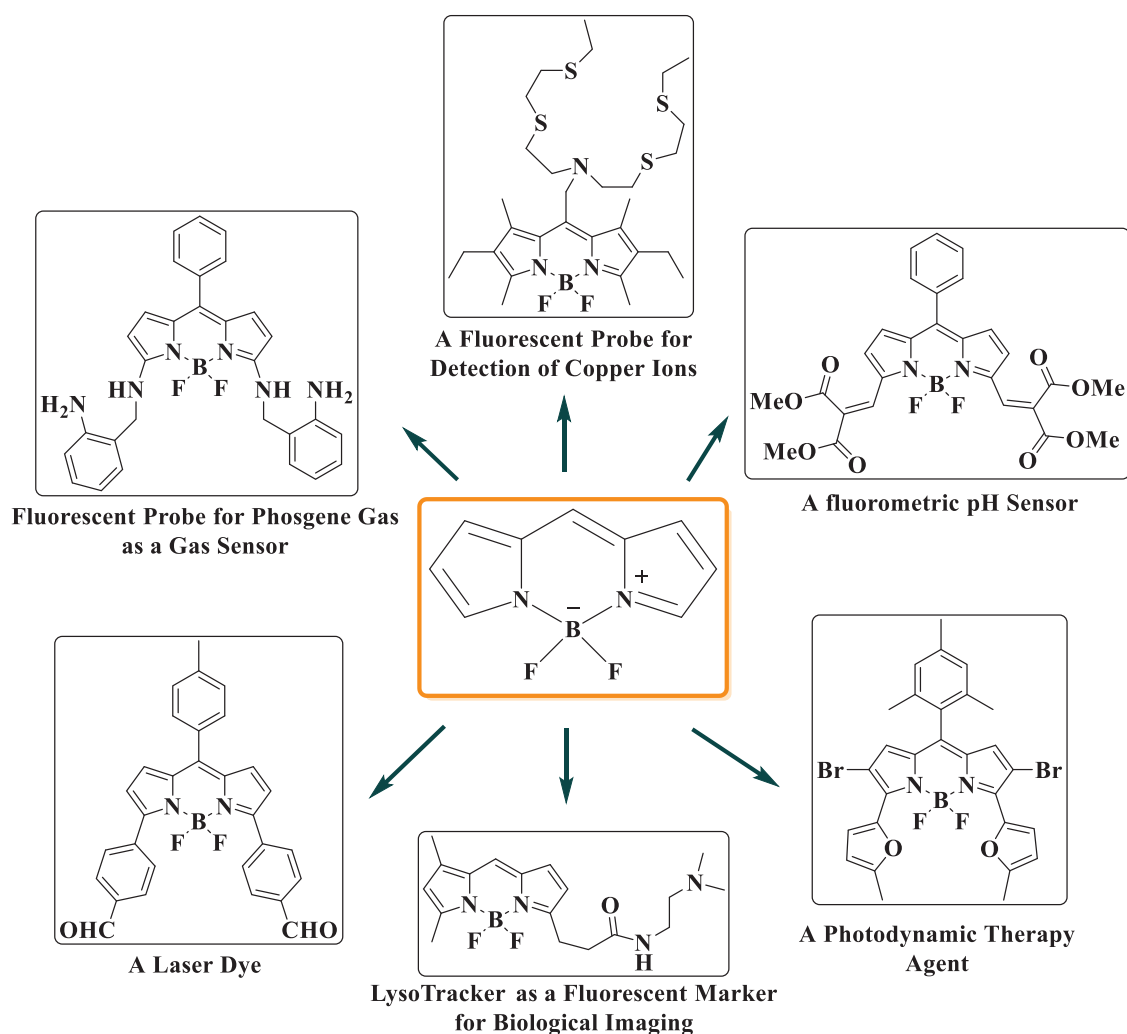
Figure 1.5. Diagram of some of the BODIPY derivatives considered for each of the application fields discussed

## 1.3. The Sensing Mechanism: ICT

Numerous photophysical mechanisms such as photoinduced electron transfer (PET) and intramolecular charge transfer (ICT) have been used to explain changes in fluorescence, including absorbance spectra, emission spectra, quantum yield, and fluorescence lifetimes. One of the most common sensing mechanisms used in designing fluorescent chemosensors is the intramolecular charge transfer (ICT) mechanism. In the design of ICT-based fluorescent probes, a linker is not used and a fluorophore unit is connected directly to a receptor unit. The mechanism consists of an electron-poor site (acceptor) and electron-rich site (donor) that together create a π-electron conjugation system, which results in bathochromic shifts or hypsochromic shifts in absorbance and

emission spectra. If the donor site (e.g. the N group) coordinates with a targeted analyte, then its electron-donating character decreases, which produces a blue shift in the electromagnetic spectrum. By contrast, the binding of the acceptor unit with the analyte (e.g. the carbonyl group) promotes the electron withdrawing character of the unit and, in turn, a redshift in the spectra. The ICT mechanism can also reduce the basicity of the donor amine group and, thus result in pH-independent fluorescent probes for detection (Callan et al., 2005; Liu et al., 2013)
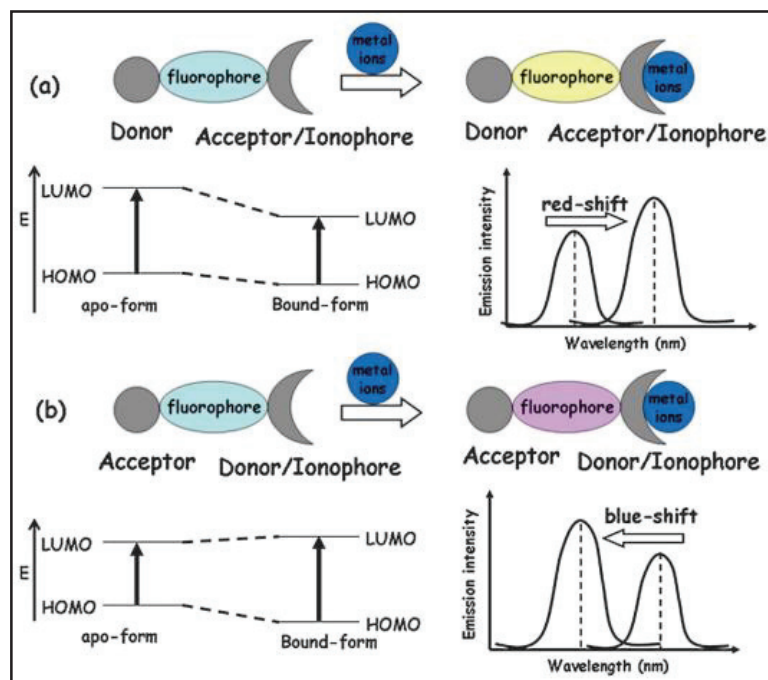


Figure 1.6. Illustration of ICT-based fluorescent probes for metal species and their ratiometric sensing mechanisms (Source: Liu et al., 2013)

## 1.4. Literature Work

Recently, the detection of cadmium ions has been of great interest. As a result, considerable researches have been reported about this issue. The most preferred design for the fluorescent probes is the complexation-based design strategy established on the non-covalent interaction such as van der Waals, electrostatic, hydrogen-bonding between receptor unit and targeted metal species. At the same time, it can be seen that the sensing mechanism is reversible if an analyte with a high affinity from the receptor is introduced to the medium. However, the major drawback of this strategy is that the metals with similar electronic, chemical and structural characteristics show cross affinity, so the probe

exhibit low selectivity against several metal ions. For example, it is challenging to distinguish Cd ions from Hg, and Cu, and mostly Zn ions.

For the first time, Liu and colleagues announced a small molecule based on the fluorescein dye and thiosemicarbazide as selective for only cadmium ions. This sensor exhibited selectivity to Cd ions in the HEPES buffer solution. The fluorescence intensity of the probe increased 2.5 fold in the presence of $Cd^{2+}$. Enhanced fluorescence is due to the formation of Cd ions and the probe complex with a 1:1 formation ratio. The increase in the fluorescence intensity occurred because the rotation of the acyclic C=N bond in the structure was inhibited after the complexation of Cd with the probe. Also, this sensor was applied to HK-2 cell lines. They studied with the micromolar concentration of Cd ions at 480 nm as excitation wavelength and 521 nm as emission wavelength (Liu et al., 2007)
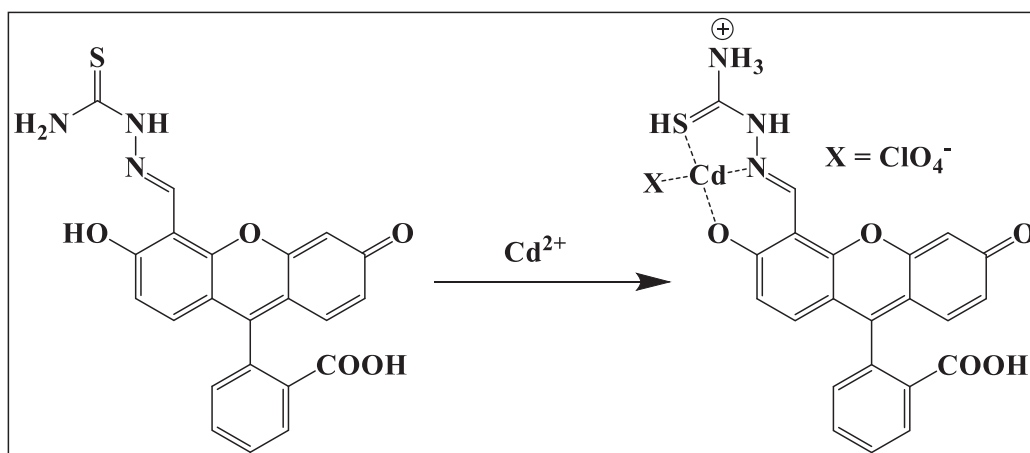


Figure 1.7. Proposed structures for Liu-1 in the presence and absence of $Cd^{2+}$
(Source: Liu et al., 2007)

In the same year, Peng et al. reported the first selective BODIPY-based fluorescent probe in living cells. They used N, N-bis(pyridine-2-ylmethyl)benzene-amine as a receptor unit and vinyl bond between BODIPY and the receptor led to shifted emission. It is based on the internal charge transfer mechanism and also ratiometric responses in fluorescence emission spectra. The maximum emission wavelength of the free probe is observed at 656 nm with 12% quantum yield whereas at 579 nm upon addition of $Cd^{2+}$ with 59% quantum yield. The probe was applied to PC12 and DC cells in the presence of micromolar of $Cd^{2+}$ (Peng et. al., 2007).
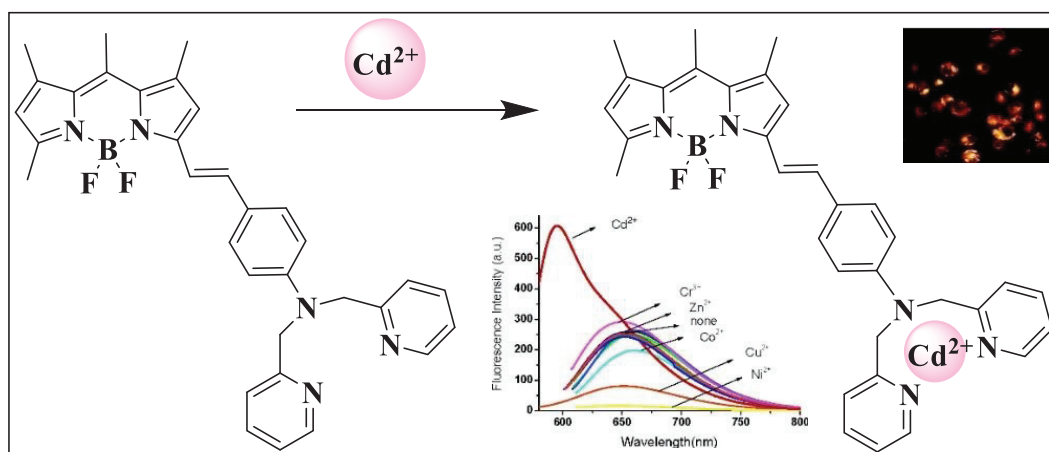
Figure 1.8. The proposed sensing mechanism of the Peng-Cd-1
(Source: Peng et. al., 2007)

In 2009, Xue published a fluorescent sensor (QA) based on acetamidoquinoline with Di-(2-picolyl)amine (DPA) as a receptor unit for detection of Cadmium and Zinc ions. They studied with aqueous buffer solution (10 mM Tris-HCl, 20% DMSO, 0.1 M KNO$_3$, pH=7.4). The coordination confirmations in sensing Zn$^{2+}$ and Cd$^{2+}$ showed differences. DPA and 8-position amide coordinate with Cd ions without deprotonation whereas Zn ions bound the 8-position N atom stronger and in this way N atom deprotonated. Free QA showed a faint fluorescence emission at 389 nm and a spectral slight emission shift occurred after binding Cd ions with fluorescence intensity at 422 nm and 40-fold enhancement referring to PET mechanism. In contrast, after complexation with Zn$^{2+}$, the fluorescence intensity only increased 2-fold. However, the emission spectra had a distinct red-shift indicating the ICT mechanism with maximum fluorescence intensity near 490 nm (Xue et al., 2009).
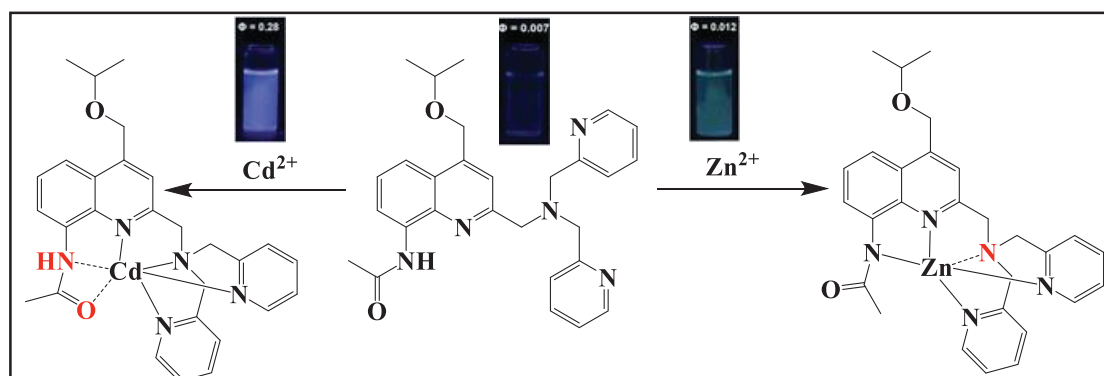


Figure 1.9. Proposed coordination conformation for QA with Cd$^{2+}$ and Zn$^{2+}$ sensing with visible emission observed in the absence and presence of Cd$^{2+}$ and Zn$^{2+}$
(Source: Xue et al., 2009)

In 2012, a quinoline-based fluorescent probe (APQ) for detection of Cadmium ions in vitro and in vivo was reported by Li and colleagues. APQ indicated high ion selectivity

and sensitivity for $Cd^{2+}$. The probe was constructed by 6-substituted quinoline as the fluorophore and $N^1,N^1$-dimethyl-$N^2$-(pyridin-2-ylmethyl)ethane-1,2-diamine group as the receptor unit. Also, a 4-methoxyphenylvinyl conjugation-enhancing group has introduced the structure to promote intramolecular charge transfer (ICT). Tris-HCl (50 mM, pH = 7.4) ethanol–$H_2O$ (v/v = 1:9) buffer was used to spectroscopic measurements. APQ exhibited a faint emission response ($\Phi_{free}$ = 0.057) at 475 nm and APQ-$Cd^{2+}$ complex showed 4-fold emission increment ($\Phi_{Cd2+}$ = 0.2124) at the 520 nm with a red-shift by binding mode 1:1. Additionally, cytotoxicity assays with HeLa cells showed that APQ was permeable (Li et al., 2012).
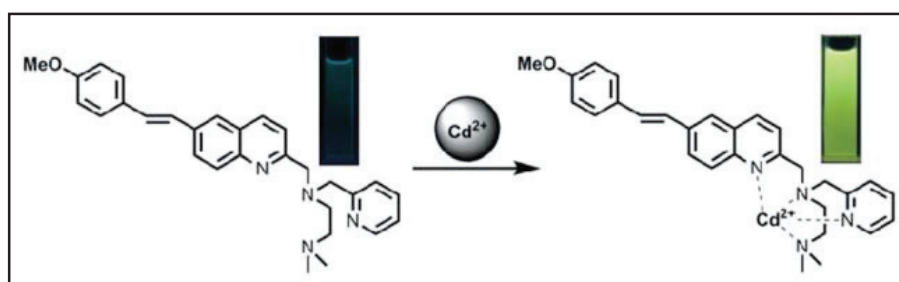


Figure 1.10. The design of APQ for $Cd^{2+}$ detection (Source: Li et al., 2012)

In 2016, Qin et al. announced a metal ion-sensitive fluorescent probe on the BODIPY platform coupled at the 3-position to a DPA as a chelator and at the 5-position to a phenylethynyl. Because of the phenyl-ethynyl species, it red-shifted compared to unsubstituted BODIPY core. They studied the complexation of the probe (Qin-1) with various metal ions. Qin-1 formed 1:1 complexes with several transition metal ($Ni^{2+}$, $Cu^{2+}$, $Zn^{2+}$) and heavy metal ($Cd^{2+}$, $Hg^{2+}$) ions. It produced bathochromic shifts in the absorption and emission spectra.
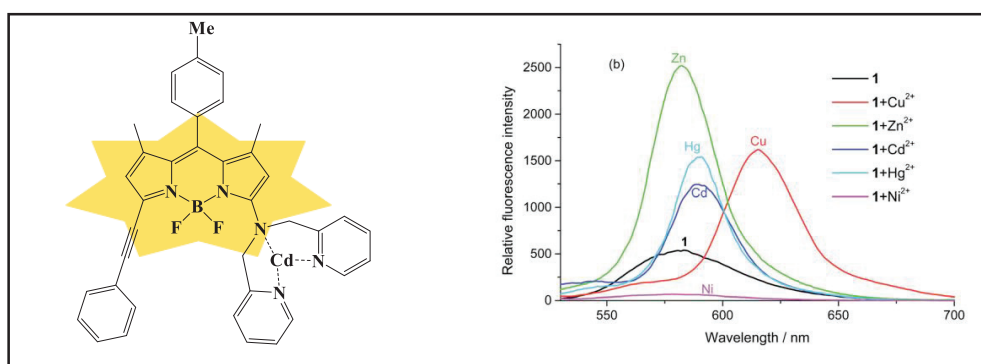


Figure 1.11. Complex of the Qin-1 with $Cd^{2+}$ and its fluorescence emission spectra in the presence of the transition metal ions $Cu^{2+}$ (60 mM), $Zn^{2+}$, $Ni^{2+}$, and the heavy metal ions $Cd^{2+}$ and $Hg^{2+}$ in acetonitrile (Source: Qin et al., 2016)

In 2017, Me$_4$BOPHY based fluorescent probe (Cheng-1) was announced sensing with an ICT mechanism. As an electron moiety, *N,N*-bis(pyridin-2-ylmethyl)benzenamine (BPA) was used. After coordination of Cd with Cheng-1, the electron-donor ability of BPA was eliminated resulting in a blue shift of the emission and absorption spectra. The free probe has emission maxima at 675 nm, and the coordinated probe has emission maxima at 570 nm. Also, the color of the solution changed from red to fluorescent yellow by the observed naked eye. Although Cheng-1 has a fluorescence response to Zn$^{2+}$, it has still emission maxima at 675 nm. Therefore, Cheng-1 is a selective probe for Cd ions (Cheng et al., 2017).
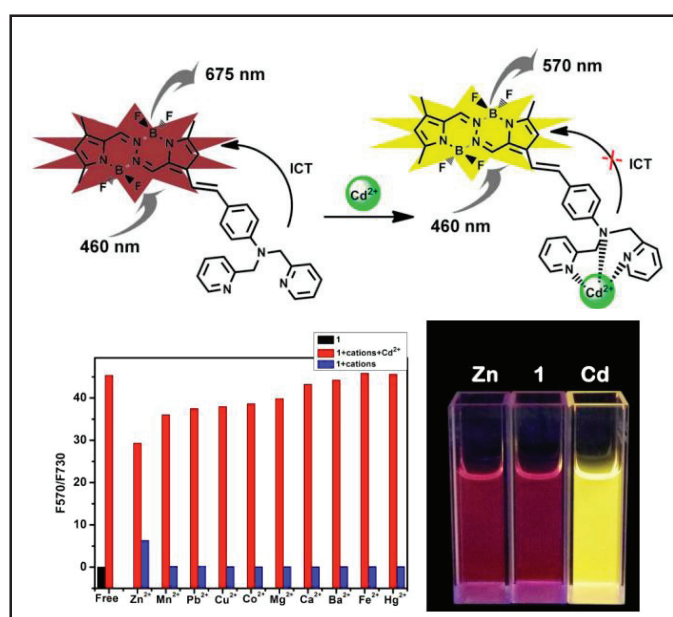


Figure 1.12. The sensing mechanism of Cheng-1 towards Cd ions (up). The fluorescence intensity ratio of Cheng-1 for various metal species in acetonitrile and observed fluorescence responses of Cheng-1 for Zn$^{2+}$ and Cd$^{2+}$ (bottom) (Source: Cheng et al., 2017).

As a more recent study, Maity et al. reported a water-soluble and reversible BODIPY based fluorescent probe (LiBDP) for the detection of Cd$^{2+}$ in 2019. BODIPY dye was used as a fluorophore and dicarboxylate pseudo-crown ether as a coordinating site. Its sensing mechanism relied on the PET mechanism. LiBDP was selective for Cd ions over the other metal species indicating 1:1 binding stoichiometry in aqueous media. LiBDP had weak emission spectra with 0.057 quantum yield and after coordination of Cd with the probe emission response enhanced with the increase of the quantum yield as 0.43 via blocking of the PET process binding LiBDP through the ether-O, carbonyl-O, and amine-N. Also, it was reversible and reusable in the presence of S$^{2-}$ (Maity et al., 2019).
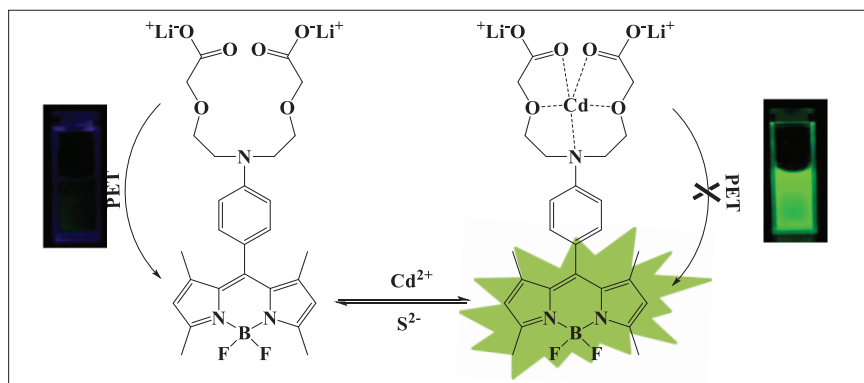
Figure 1.13. Proposed mechanism for sensing event of LiBDP with the naked-eye appearance in the absence and presence of the cadmium ions
(Source: Maity et al., 2019)

In the most recent study, Piyanuch, and colleagues published a selective aza-BODIPY based fluorescent probe (Piyanuch-1) for the detection of $Cd^{2+}$ in 2021. They studied in aqueous solution as 8:2 PBS/ACN + Triton X-100 media. Piyanuch-1 showed a color change from colorless to green with an enhancement of the fluorescence emission response at 710 nm. The probe was designed via a PET mechanism indicating a turn-on fluorescent switch. Furthermore, Piyanuch-1 was operated in the imaging of Cadmium ions in the HEK-293 cell line. It showed that the probe can be utilized for the determination of $Cd^{2+}$ in living cells (Piyanuch et al., 2021).
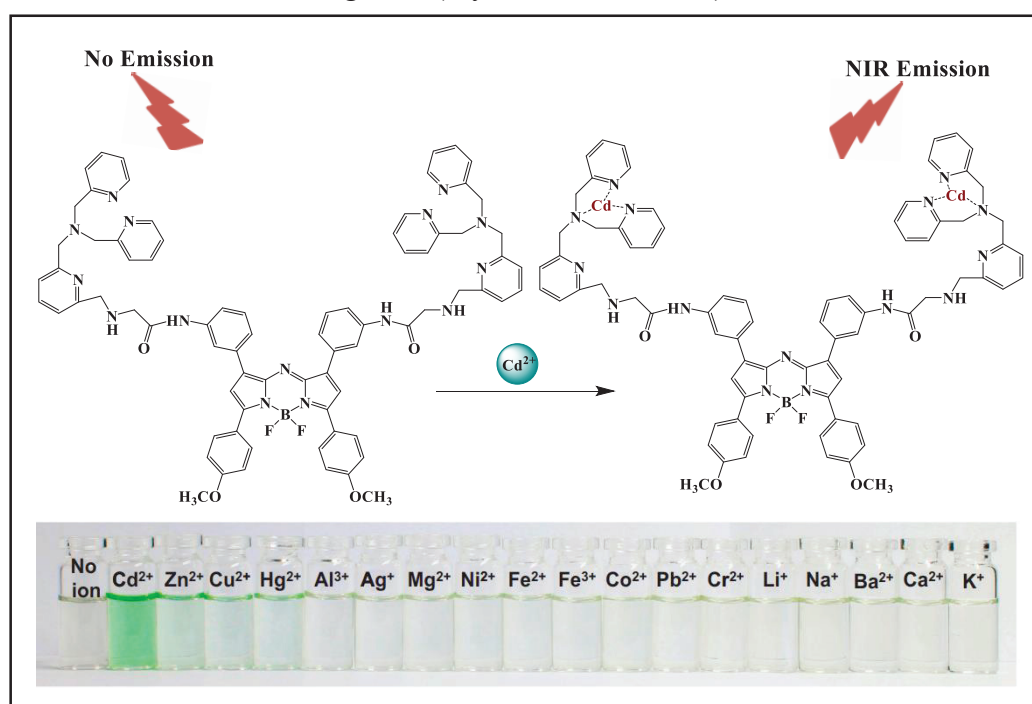


Figure 1.14. Proposed mechanism for coordination of $Cd^{2+}$ with Piyanuch-1 and chromogenic change of Piyanuch-1 in the presence of different cations
(Source: Piyanuch et al., 2021)

# CHAPTER 2

# EXPERIMENTAL STUDY

## 2.1. General Methods

All reagents were purchased from commercial suppliers (Aldrich and Merck) and used without further purification. All reactions were carried out under a nitrogen atmosphere. $^1$H NMR and $^{13}$C NMR were measured on a Varian VNMRJ 400 Nuclear Magnetic Resonance Spectrometer. UV absorption and fluorescence emission spectra were obtained on Horiba Duetta, the two-in-one Fluorescence, and Absorbance Spectrometer. Samples were contained in quartz cuvettes with a path length of 10.0 mm (2.0 mL volume). Upon excitation at 460 nm, the emission spectra were integrated over the range 480 nm to 750 nm with a slit width of both excitation and emission 3 nm / 3 nm. pH was recorded by the HI-8014 instrument (HANNA). The fluorescence images were obtained through a Zeiss fluorescence microscope (Zeiss Axio Observer). The solutions of metal ions were prepared from $HgCl_2$, KCl, $ZnCl_2$, $CrCl_2$, $CdCl_2$, NaCl, $CuCl_2$, $CoCl_2.6H_2O$, $BaCl_2.H_2O$, $NiCl_2.6H2O$, LiCl, $Pb(NO_3)_2$, $Mn(SO_4).H_2O$, $Al(NO_3)_3.9H_2O$, $Fe(NO_3)_3.9H_2O$, $Mg(NO_3)_2.6H_2O$, $AuCl_3$, and AuCl in EtOH and(or) $H_2O$.

## 2.2 Determination of Detection Limit

The detection limit was calculated from the following equation (Maity et al., 2019):

$$\textbf{Detection Limit} = \textbf{3σbi/m}$$

where σbi is the standard deviation of the blank solution, m is the slope between fluorescence intensity versus sample concentration. For the calculation of the detection limit, fluorescent titration data were used. Also, the emission intensity of probe molecules

without metal ions was measured by 10 times and the standard deviation of blank measurements was determined to detect the signal/noise ratio. The detection limit was then calculated with the given equation.

## 2.3 Determination of Quantum Yields

Fluorescence quantum yields of synthesized probe molecules in the presence and absence of metal ions were determined. Rhodamine B dye ($\Phi$=0.31 in water) was used as the reference. The reference and sample concentrations were adjusted to acquire an absorbance of 0.1 or less. The quantum yield was calculated according to the following equation (Arbeloa et al., 1989):

$$\Phi_S = \Phi_R \, (A_S/A_R) \, (ABS_R/ABS_S) \, (n_S/n_R)^2$$

Here $\Phi$ is the fluorescence quantum yield, (ABS) is the absorbance at the excitation wavelength, A is the area under the corrected emission curve, and n is the refractive index of the solvents used. The subscripts R and S represent the reference and the sample, respectively.

## 2.4. Determination of Association Constants

The association constants ($K_a$) of metal ions ($Cd^{2+}$) were determined based on the fluorescence titration data using the equation (Bandyopadhyay et al., 2012);

$$(F - F_0) = \Delta F = [M^{2+}] \, (F_{max} - F_0) \, / \, (K_d + [M^{2+}])$$

$K_d$ is the dissociation constant, $F_0$ and $F_{max}$ are the fluorescence intensities of the probe alone and high concentration of $Cd^{2+}$, respectively. F is the fluorescence intensity with an obtained concentration of $Cd^{2+}$. The Benesi-Hildebrand Plots of $1 / \Delta F$ against $1/[Cd^{2+}]$ are used for the determination of binding constants in the ACN/PBS system (8:2, v/v) and only ACN. According to the linear equation $Y = MX + B$, $K_d$ is calculated from the ratio M/B ($K_d$=$1/K_a$).

## 2.5. Cell Imaging

A549 Human Lung Adenocarcinoma cell lines were grown in DMEM supplemented with 10% FBS (fetal bovine serum) in an atmosphere of 5 % $CO_2$ at 37 °C. The cells were plated on 12 mm cover glasses in a 6-well plate and left to grow for 24h. The cells were incubated with probe molecule (20 µM), $Cd^{2+}$ (200 µM), and DAPI for 20 min at 37 °C, sequentially. Before, between, and after incubation processes, the cells were washed with PBS three times. Lastly, the fluorescence cell images were acquired through the fluorescence microscope.

## 2.6. Synthesis Section

The synthesis route for **BOD-MRY** was demonstrated in Figure 2.1. BOD-1, BOD-2, BOD-3, and **BOD-MRY** were synthesized by using the literature procedures.
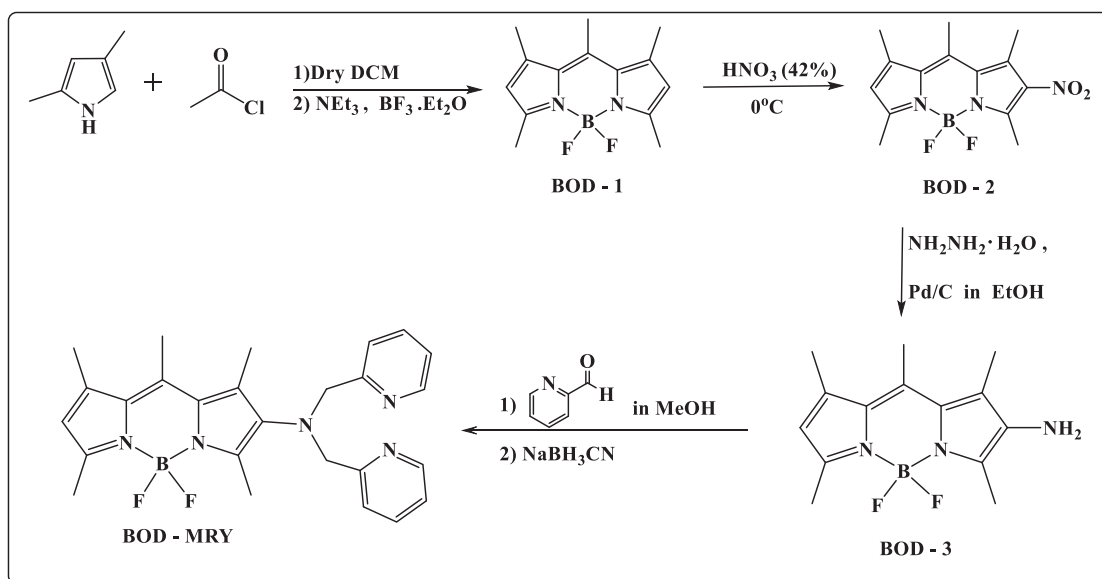


Figure 2.1. Stepwise Synthesis of **BOD-MRY**

As indicated in Figure 2.1.**, BOD-MRY** was prepared according to the synthesis pathway. Firstly, the nitro group was introduced to BOD-1 to obtain BOD-2 by exploiting nitric acid. Then, BOD-3 as an amine derivative -connected to directly BODIPY core with the 2-position- was achieved with a reduction reaction of BOD-2. Lastly, **BOD-MRY** was synthesized by using 2-pyridine carboxaldehyde moiety.

## 2.6.1. Synthesis of BOD-1
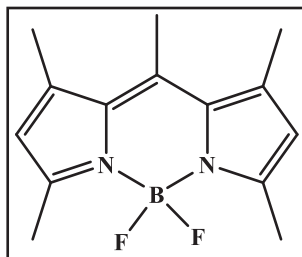


Figure 2.2. Structure of 5,5-difluoro- 1,3,7,9,10- pentamethyl- 5H-4$\lambda^4$,5$\lambda^4$-dipyrrolo [1,2-c:2',1'-*f*] [1,3,2] diazaborinine  (BOD-1)

**5,5-difluoro-1,3,7,9,10-pentamethyl-5H-4$\lambda^4$,5$\lambda^4$-dipyrrolo[1,2-c:2',1'-*f*][1,3,2] diazaborinine  (BOD-1)** was synthesized according to the literature procedure (Niu et al., 2019). 0.4 mL of 2,4-dimethylprrole (3.7 mmol) was dissolved in 2.0 of dry DCM and added 6.4 mL of acetyl chloride (9.1 mmol) to the solution drop by drop at room temperature (RT). After that, the solution was heated to reflux for 1 hour at 40 °C, then cooled to RT. After cooling, 17-20 mL of n-hexane was poured onto the mix. and it was transferred to a new flask. Then, the solvent of the mixture was removed at a rotary evaporator. It was used for the next step without further purification. The resulting compound was dissolved in 18 mL of dry DCM, then added 1.55 mL of dry Et$_3$N (11.1 mmol) by a dropping funnel. The solution was stirred for 15 minutes. After that, 2.06 mL of BF$_3$.Et$_2$O (16.7 mmol) dropwise and stirred at RT for 1 hour. The final product was extracted with DCM and saturated H2O/Na$_2$CO$_3$. The organic phase was dried over anhydrous magnesium sulfate (MgSO$_4$) and concentrated in a vacuum. The crude product was purified by column chromatography using silica gel (12:1, Hexane: Ethyl Acetate) to afford BOD-1 as a dark-orange solid (480 mg, 49% yield). ^{1}H NMR (400 MHz, CDCl$_3$) $\delta_H$: 5.98 (s, 2H), 2.49 (s, 3H), 2.44 (s, 6H), 2.33 (s, 6H).

## 2.6.2. Synthesis of BOD-2
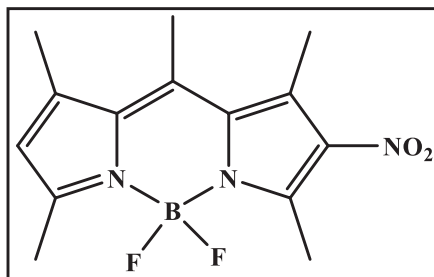


Figure 2.3. Structure of 5,5-difluoro-1,3,7,9,10-pentamethyl-2-nitro5H-5$\lambda^4$,6$\lambda^4$ dipyrrolo[1,2-c:2',1'*f*][1,3,2]diazaborinine (BOD-2)

**5,5-difluoro-1,3,7,9,10-pentamethyl-2-nitro5H-5$\lambda^4$,6$\lambda^4$-dipyrrolo[1,2-c:2',1'*f*] [1,3,2]diazaborinine (BOD-2)** was synthesized by using literature procedure (Ray et al., 2017). Two necked-balloon was charged with 130 mg of BOD-1 (0.50 mmol). Cooled to 0 °C of nitric acid (11 mL, 42%) was added to the balloon, and the orange mixture was stirred at 0 °C in an ice bath for 1.5 hours. The progress of the reaction was monitored by thin-layer chromatography (TLC). After the reaction was done, the mixture was extracted with DCM and dried over $MgSO_4$. The solvent was removed by rotary evaporation. The synthesized product as orange needles, BOD-2, was used for the next step without further purification method (140 mg, 90% yield). $^1$H NMR (400 MHz, CDCl$_3$) $\delta_H$: 6.29 (s, 1H), 2.80 (s, 3H), 2.71 (s, 3H), 2.70 (s, 3H), 2.59 (s, 3H), 2.49 (s,3H).

## 2.6.3. Synthesis of BOD-3
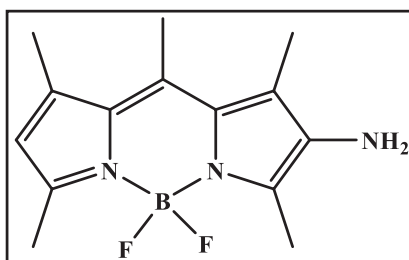


Figure 2.4. Structure of 5,5-difluoro-1,3,7,9,10-pentamethyl-5H5$\lambda^4$,6$\lambda^4$-dipyrrolo[1,2-c:2',1'-*f*][1,3,2] diazaborinin-2-amine (BOD-3)

**5,5-difluoro-1,3,7,9,10-pentamethyl-5H5$\lambda^4$,6$\lambda^4$-dipyrrolo[1,2-c:2',1'-*f*][1,3,2] diazaborinin-2-amine (BOD-3)** was obtained according to the literature procedure (Emrullahoğlu et al., 2018). To solution of BOD-2 (140 mg, 0.45 mmol) in 10 mL of EtOH, Pd/C (57.5 mg, 0.54 mmol) and $NH_2NH_2.H_2O$ (0.5 mL, 10.3 mmol) were added respectively. The reaction mixture was heated to reflux temperature for 2 hours. After that, it was cooled to room temperature and filtered through celite using DCM. The solvent was removed under reduced pressure. The resultant residue was purified by column chromatography on silica gel (2:1, Hexane: EtOAc) to afford BOD-3 as a purple solid (50 mg, 40% yield). $^1$H NMR (400 MHz, CDCl$_3$) $\delta_H$: 7.19 (s, 2H), 5.88 (s, 1H), 2.46 (s, 3H), 2.40 (s, 6H), 2.30 (s, 3H), 2.15 (s, 3H).

## 2.6.4. Synthesis of BOD-MRY
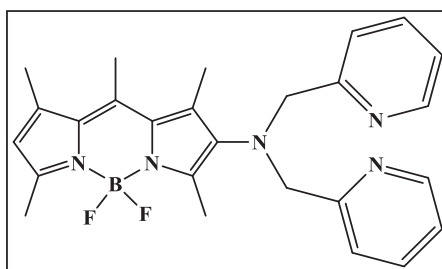


Figure 2.5. Structure of 5,5-difluoro-1,3,7,9,10-pentamethyl- N,N- bis(pyridin-2-ylmethyl)- 5H-5$\lambda^4$,6$\lambda^4$- dipyrrolo [1,2-c:2',1'-*f*] [1,3,2] diazaborinin-2-amine **(BOD-MRY)**

**5,5-difluoro-1,3,7,9,10- pentamethyl-N,N- bis(pyridin-2-ylmethyl)- 5H-5$\lambda^4$,6$\lambda^4$-dipyrrolo[1,2-c:2',1'-*f*][1,3,2]diazaborinin-2-amine (BOD-MRY)** was synthesized based on the literature procedure (Sahli et al., 2011). 50 mg of BOD-3 (0.18 mmol) was dissolved in MeOH (4 mL). Then, 2-pyridine carboxaldehyde (68.5 µL, 0.72 mmol) was introduced to the medium. The reaction was carried out overnight at RT under dark conditions. After overnight stirring, sodium cyanoborohydride (45 mg, 0.72 mmol) was added to the mixture, it was stirred for 4 hours at RT. Extraction was carried out with DCM and water, and the organic phase was dried over with MgSO$_4$. The solvent was evaporated, and the crude product was purified by column chromatography using silica gel (50: 1, DCM: MeOH) to afford **BOD-MRY** as a dark-pink solid (25 mg, 30% yield). $^1$H NMR (400 MHz, CDCl$_3$) $\delta_H$ 8.45 (s, 2H), 7.55 (s, 2H), 7.29 (s, 2H), 7.08 (s, 2H), 5.92

(s, 1H), 4.28 (s, 4H), 2.43 (s, 3H), 2.40 (s, 3H), 2.29 (s, 3H), 2.24 (s, 3H), 2.15 (s, 3H). $^{13}$C NMR (101 MHz, CDCl$_3$) $\delta_C$: 158.79 (s), 152.92 (s), 152.62 (s), 149.05 (s), 140.91 (s), 140.68 (s), 140.27 (s), 136.39 (d, J = 8.1 Hz), 131.89 (s), 130.02 (s), 123.12 (s), 122.15 (s), 120.69 (s), 60.12 (s), 29.65 (s), 17.23 (s), 16.64 (s), 14.19 (d, J = 19.8 Hz), 12.58 (s).

# CHAPTER 3

# RESULT AND DISCUSSION

## 3.1. General Perspective

In this study, we report the design and synthesis of a novel, fast, selective, and colorimetric fluorophore derivative, **BOD-MRY**, and the evaluation of its potential use as a fluorescent probe. This probe was constructed by directly introducing two 2-pyridine carboxaldehyde units to the amine-functionalized boron–dipyrromethene (BODIPY) fluorophore moiety, without using spacer or linker, it is expected to use for the detection of cadmium ions over the other competitive metal ions in living cells.

Herein, we select the BODIPY skeleton as fluorophore due to its remarkable photophysical features as well as for its ease of chemical modification. Based on the literature studies, we use Di-(2-picolyl)amine (DPA) as a suitable recognition site by attaching two 2-pyridine carboxaldehyde to free amine of the BODIPY. As far as we know, it was the first time that substituted the DPA unit to 2-position of the BODIPY core directly without any bridges.

As demonstrated in Figure 3.1., the fluorescence emission of free **BOD-MRY** was quenched by the ICT mechanism. Directly 2-position amine-functionalized on the BODIPY dyes is known for intramolecular charge transfer representing the amino group as the strong electron-donating site and BODIPY core as the electron acceptor site. The electron donation is provided by a lone pair electron of the nitrogen. After introducing $Cd^{2+}$ to the **BOD-MRY**, the ICT mechanism is diminished and fluorescence emission enhancement is observed (Alnoman et al., 2017). Colorimetric changes of the probe can be monitored from non-fluorescent pink to fluorescent green color.
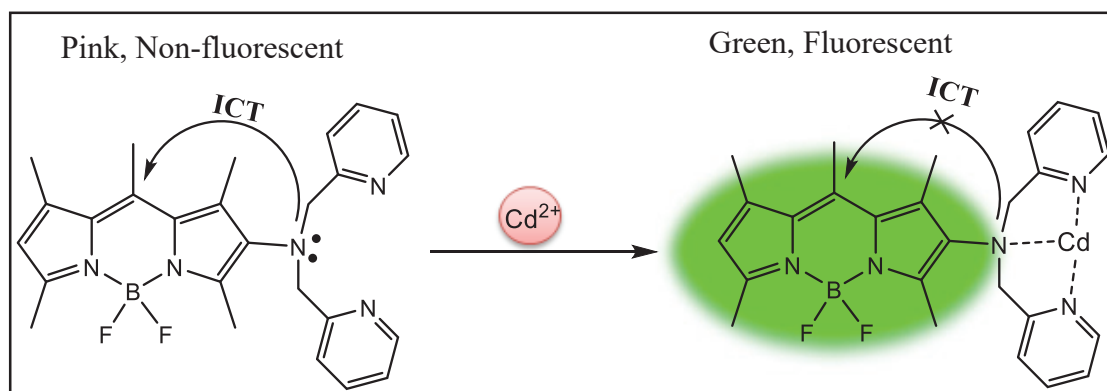
Figure 3.1. Coordination-based detection of cadmium with **BOD-MRY**

In this chapter, all performing spectroscopic analyses and cell studies to measure the photophysical and spectroscopic behaviors of **BOD-MRY** are explained.

## 3.2. Spectroscopic Measurements

The investigation was started with the determination of the optimum conditions for the sensing process. Firstly, the optical behavior of **BOD-MRY** was investigated in different organic solvents, such as EtOH/H$_2$O (v/v, 8:2, pH = 7.0), ACN/ H$_2$O (v/v, 8:2, pH = 7.0), DMF/ H$_2$O (v/v, 8:2, pH = 7.0), and DMSO/ H$_2$O (v/v, 1:100, pH = 7.0). The highest fluorescent response was observed in ACN/ H$_2$O (v/v, 8:2, pH = 7.0) system. (Fig. 3.2.) Next, various buffer solutions which are HEPES, PBS, and Phosphate buffer solutions were examined. Also, the effect of water content with variations was investigated (Fig. 3.3.). Eventually, the most favorable condition for recognition of Cd$^{2+}$ ions was adjusted as 0.1 M PBS buffer solution/ACN (2:8, v/v) at pH = 7.0 with 20 μM dye and 50 equivalents cadmium concentrations.
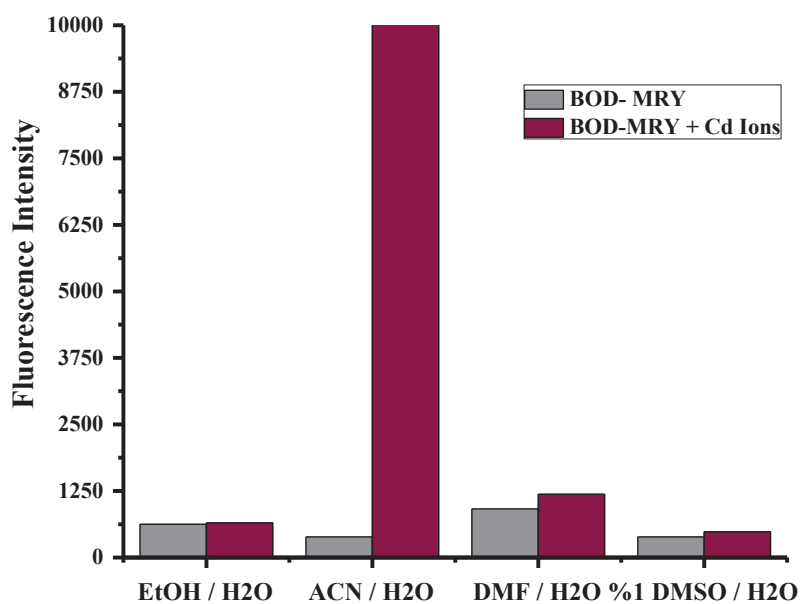
Figure 3.2. Effect of solvent on the interaction of **BOD-MRY** (20.0µM) with/without $Cd^{2+}$ (50 eq.) in various solvent combinations (Solvent/H$_2$O, 8:2, v/v) ($\lambda_{ex}$: 460 nm, $\lambda_{em}$ = 480 – 750 nm) (pH = 7.0)
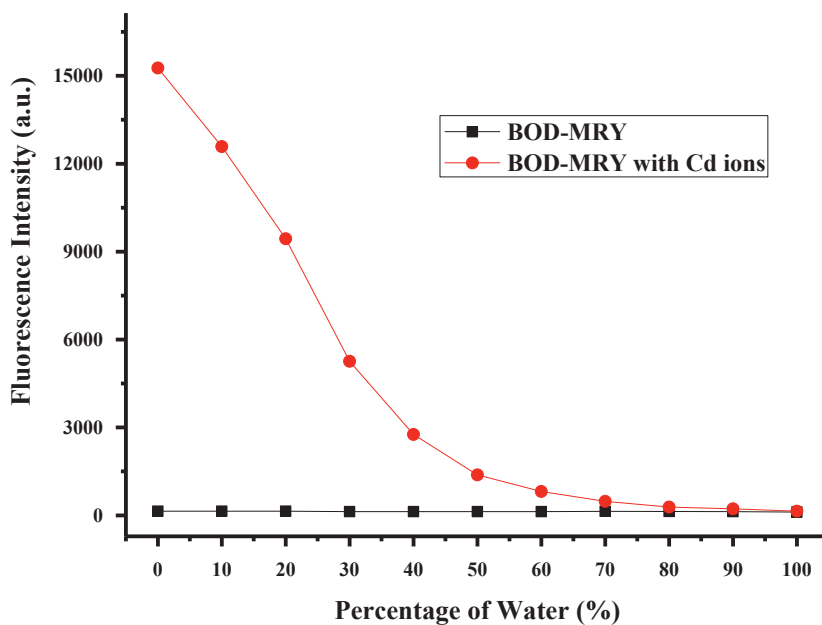


Figure 3.3. Effect of water on the interaction of BOD-MRY (20.0 µM) with/without $Cd^{2+}$ (50 eq.) in various fraction of PBS (ACN/PBS) ($\lambda_{ex}$: 460 nm, $\lambda em$ = 480 – 750 nm) (pH = 7.0)

To find out the practicability of sensing events the detection manner and biological application of **BOD-MRY** were examined in the pH range 1-9 (20 µM **BOD-MRY** in ACN/HEPES, 8:2, v/v). As demonstrated in Fig. 3,4., in the absence of Cd ions, there is no significant fluorescence change of the probe between pH 1 and 9. However, with the promotion of $Cd^{2+}$, high fluorescence responses clearly showed for all pH values reported, except pH 1 and 2 as acidic media. **BOD-MRY** showed the most potent fluorescence intensity change at pH 7. As seen in the results, **BOD-MRY** could be used as a probe in the pH range of 4-9. Also, the pH of the medium was established to pH 7 in all studies, which was suitable for further cell-based studies.



Figure 3.4. Emission spectra of **BOD-MRY** (20 µM) in 8:2 ACN/PBS buffer (0.1 M) at varying pH values, emission band 480-750 nm ($\lambda_{ex}$ = 460 nm) in the presence of 50.0 eq. $Cd^{2+}$

In the following step, UV-Vis absorbance and fluorescence measurements of **BOD-MRY** in the absence and presence of cadmium ions were surveyed. In the absence of $Cd^{2+}$, the probe displayed an absorption at 502 nm and absorption spectra with a minor increment, and a slight shift to 496 nm was observed in the existence of the cadmium ions (Fig. 3.5. (a)). Chromophore has a faint fluorescence emission band centered at 535 nm. In contrast, the rapid and strong fluorescence response was measured at 525 nm with a minor blue shift toward the addition of $Cd^{2+}$. The color of the solution changed from non-fluorescent pink to fluorescent green, enabling direct observation with naked eyes (Fig. 3.5.(b)).
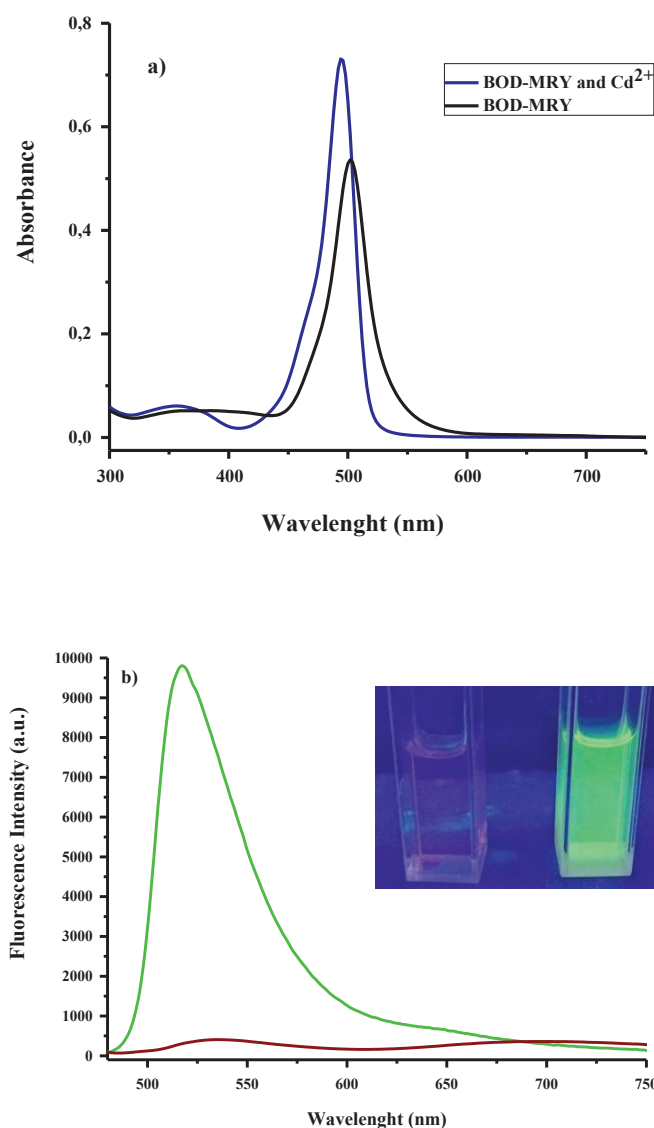
Figure 3.5. a) Absorption spectra of **BOD-MRY** (20 µM) in the presence (blue line) and absence (black line) of $Cd^{2+}$ (50.0 eq.) b) Fluorescence spectra of **BOD-MRY** (20 µM) in the absence (dark-red line) and presence (green line) of 50 eq. of $Cd^{2+}$ in 0.01 M PBS/ACN (v/v, 2:8) pH=7.0 (Inset: Naked eye appearance in the absence and the presence of cadmium ions)

Additionally, the quantum yield of **BOD-MRY** was assessed using the absorbance and emission data received before and after adding cadmium ions. As envisioned, the probe, **BOD-MRY**, is nearly non-emissive ($\Phi F= 0.0126$) due to intramolecular charge transfer (ICT) from the free, lone pair electron of nitrogen at the recognition unit. Besides, prohibition of ICT mechanism after by coordination of cadmium ions with the nitrogens of DPA led to raise in emission response and quantum yield of the coordinated fluorescent probe was measured as $\Phi F= 0.40$.

23

Moreover, selectivity studies were investigated with other metal ions which are; $Al^{3+}$, $Ba^{2+}$, $Ca^{2+}$, $Cr^{2+}$, $Cu^{2+}$, $Fe^{3+}$, $K^+$, $Li^+$, $Mg^{2+}$, $Mn^{2+}$, $Na^+$, $Ni^{2+}$, $Pb^{2+}$, $Zn^{2+}$ and $Cd^{2+}$. No substantial change in the fluorescence intensity was measured when other metal ions were added. Even for $Zn^{2+}$, which is the most competitive metal for $Cd^{2+}$, the weak response was evaluated. For the determination of interference of the other metal species over the cadmium ions, measurements were achieved as shown in Fig. 3.6. (a) and (b). These results showed that **BOD-MRY** is a highly selective and sensitive fluorescence "turn-on" probe for cadmium ions.
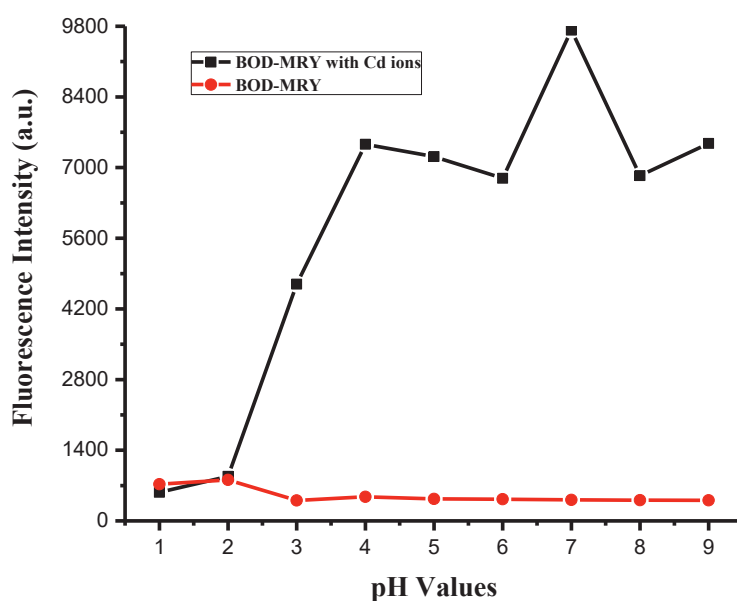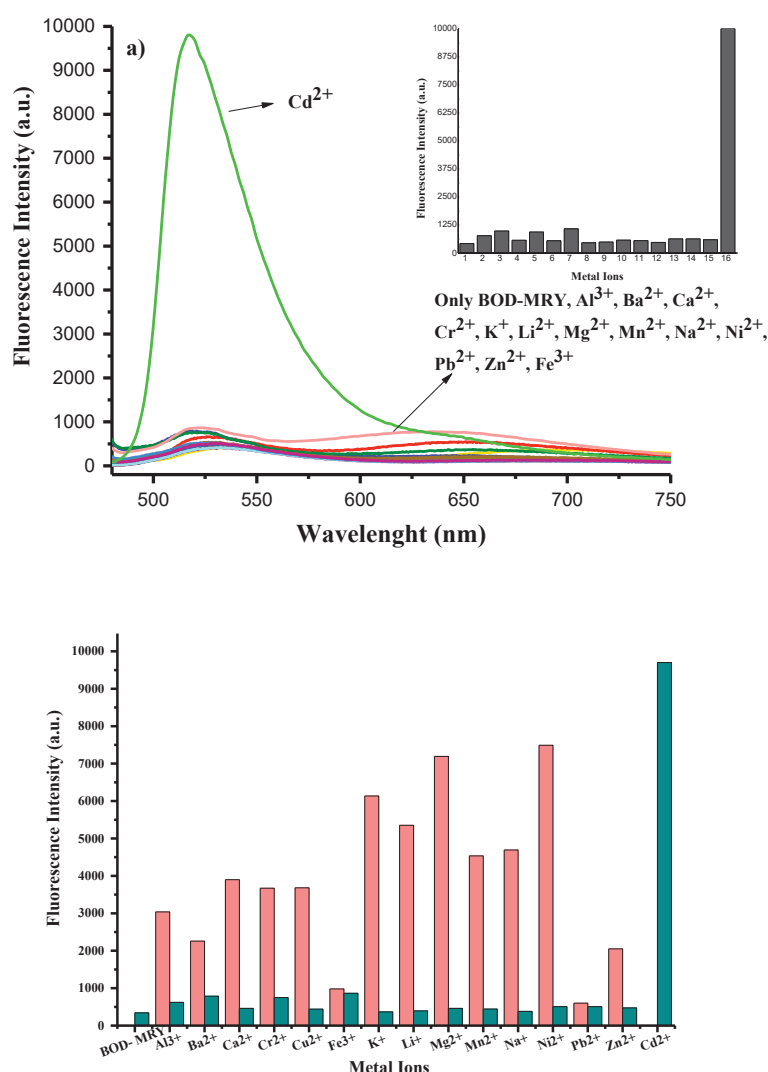


Figure 3.6. a) Emission spectra of **BOD-MRY** (20 µM) in 8:2 ACN/PBS buffer at pH=7.0, emission band 480-750 nm ($\lambda_{ex}$ = 460 nm) in the presence of 50.0 eq. cations interest (Inset: Bar graph notation)  b) Fluorescence intensities of **BOD-MRY** (20 µM) only and **BOD-MRY** (20 µM) in 8:2 ACN/PBS at pH=7.0 at $\lambda_{max}$= 525 nm in the presence of 50.0 eq. of cations interest (cyan columns) and fluorescence intensities of **BOD-MRY** (20 µM) in 8:2 ACN/PBS at pH=7.0 at $\lambda_{max}$=535 nm in the presence of $Cd^{2+}$ (50.0 eq.) and 50.0 eq. cations (pink columns)

To understand the binding ability between **BOD-MRY** and Cd ions, fluorescence titration studies were performed in both 8:2 (v/v) ACN/PBS (0.1 M, at pH=7.0) and only ACN. The studies depicted that the fluorescence intensities of the probe with the 20 μM concentration in two different media increased in direct proportion to $Cd^{2+}$ concentration. Although the fluorescence intensity of the **BOD-MRY** peaked with the addition of 20 equivalents of $CdCl_2$ in the ACN/PBS system, it reached its maximum as 10 equivalents of $Cd^{2+}$ were added in the organic medium (Fig. 3.7. (a) and (b)).
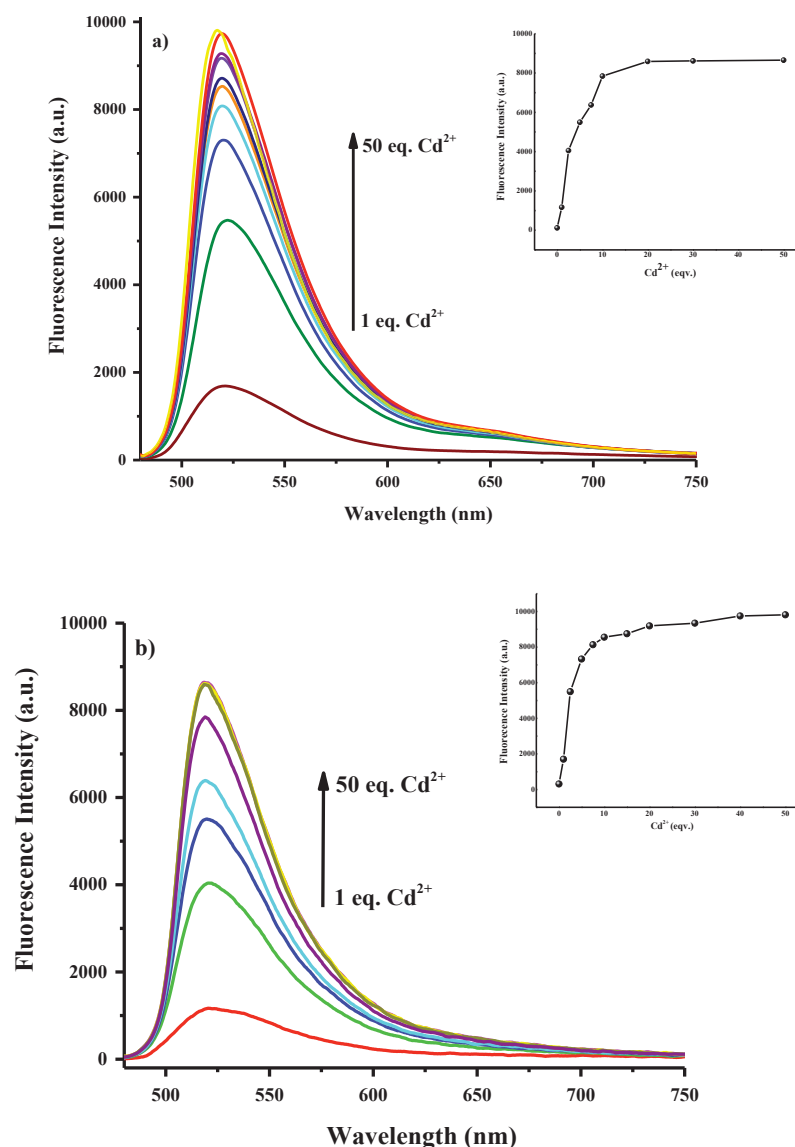


Figure 3.7. a) Change in the fluorescence spectra of **BOD-MRY** in 0.01 M PBS /ACN (pH=7.0, v/v, 2:8) upon the addition of increasing concentration of $Cd^{2+}$ (0-50 eq.) (Inset: Curve of fluorescent intensity at 525 nm versus increasing $Cd^{2+}$concentration in 0.01 M PBS buffer /ACN (pH 7.0, v/v, 2:8)) b) Change in the fluorescence spectrum of **BOD-MRY** in ACN upon the addition of increasing concentration of $Cd^{2+}$ (0-50 eq.) (Inset: Curve of fluorescent intensity at 525 nm versus increasing $Cd^{2+}$concentration in ACN)

25

In addition, the limit of detection of **BOD-MRY** was calculated to determine the minimum detectable amount of cadmium in aqueous and non-aqueous systems using the given equation in the previous chapter. The calculation was performed based on fluorescence titration. The experiments were carried out with the incremental addition of cadmium ions. As indicated in Figure 3.8, the detection limit was measured to be 279.5 nM with a linearly dependent coefficient ($R^2$) of 0.9867 in 8:2 (v/v) ACN/PBS (0.1 M, at pH=7.0), whereas its detectability in ACN was remarkably reduced and was computed as 2.2 nM ($R^2 = 0.9928$).
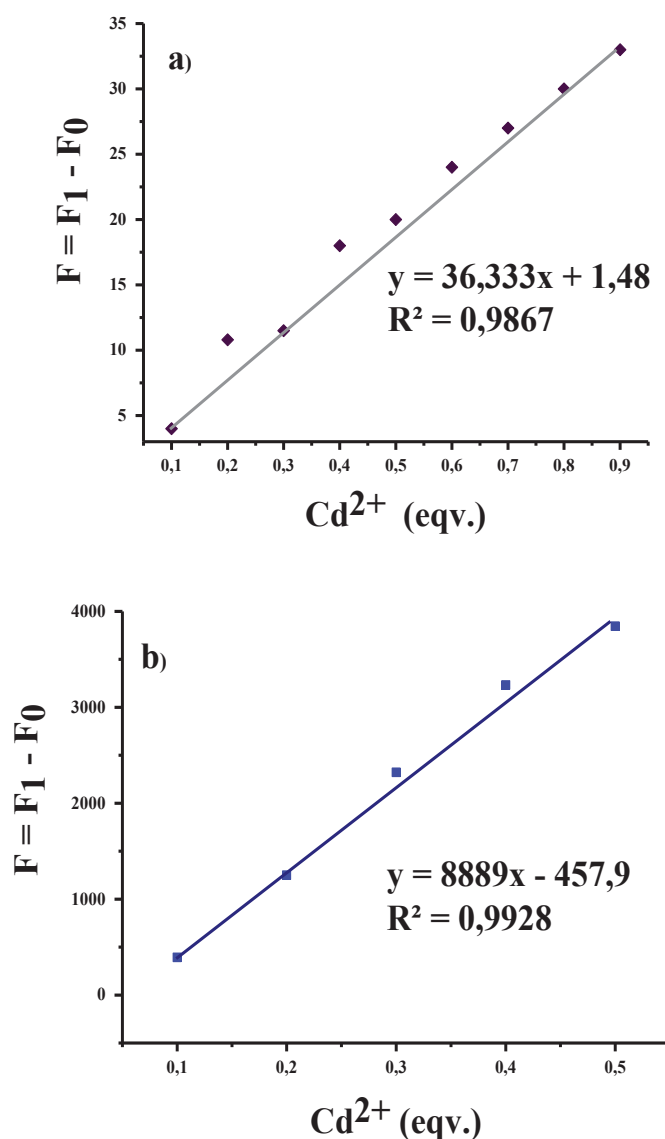


Figure 3.8. Line of detection limit: fluorescence changes of **BOD-MRY** (20 μM) at 525 nm depending on the number of equivalents of Cd ion (0 to 9 μM) a) in ACN/PBS (0.1M) (8:2 v/v, pH=7.0) b) in ACN (λex: 460 nm)

Furthermore, the interaction ability of **BOD-MRY** to $Cd^{2+}$ ions was examined by employing the Benesi-Hildebrand method and Job's plot analysis. Straight lines were obtained from the plots of $1 / \Delta F$ against $1 / [Cd^{2+}]$ in ACN, and 8:2 (v/v) ACN/PBS (0.1 M, at pH=7.0), and the related binding constants were determined as $1.3 \times 10^4$ $M^{-1}$ in organic medium and $2 \times 10^4$ $M^{-1}$ in aqueous solution (Figure 3.9. (a) and (b)). Moreover, Job's plot analysis confirmed a 1:1 stoichiometry for the complexation (Figure 3.10.).
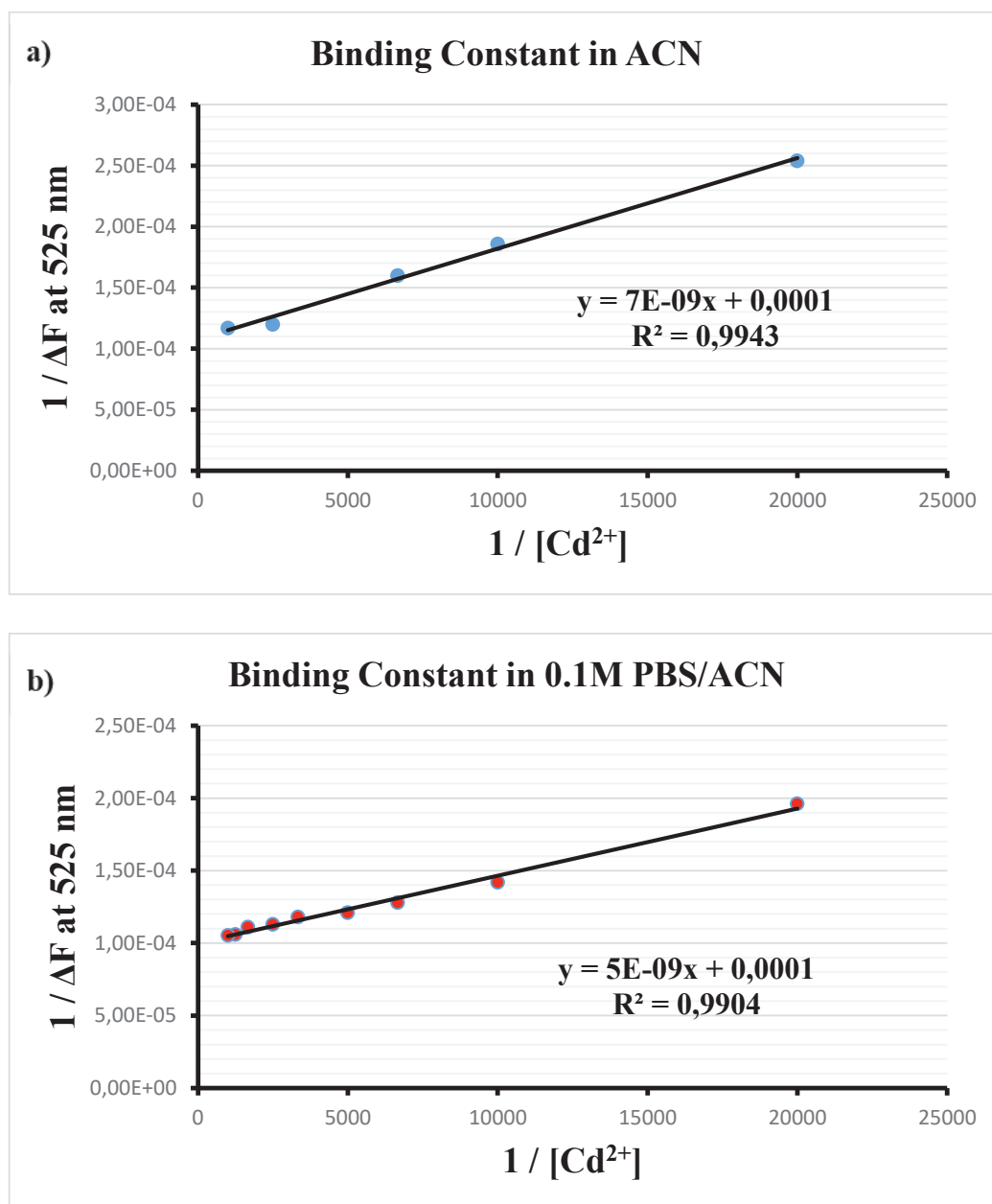


Figure 3.9. Binding ability of **BOD-MRY** to $Cd^{2+}$ a) in ACN, b) in 0.1M PBS buffer/ACN (pH=7.0, v/v, 2:8) (λex: 460 nm, λem= 525 nm )
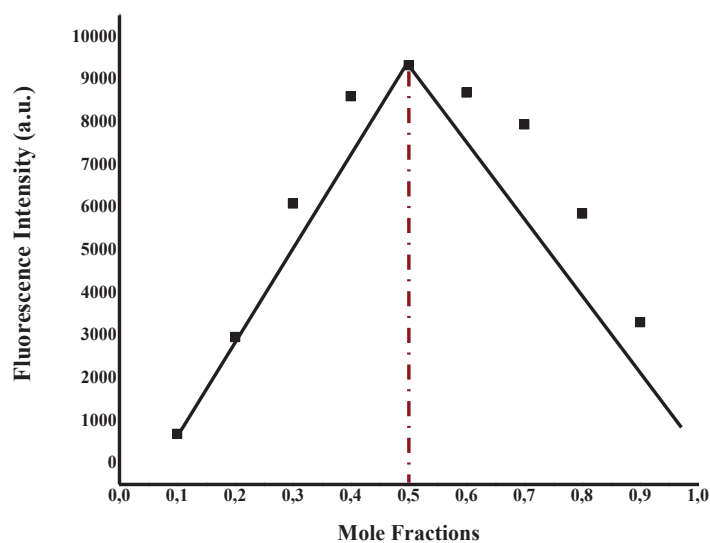
Figure 3.10. Job's plot of complexes of **BOD-MRY** and $Cd^{2+}$ in ACN with the constant total concentration of **BOD-MRY** and $Cd^{2+}$ as 50 µM ($\lambda_{ex}$= 460nm, $\lambda_{em}$= 480 – 750 nm)

As a further investigation, reversibility measurement was carried out by using CN ions. When 2 eq. of $CN^-$ was added to the solution containing 20 µM dye and 1 eq. $Cd^{2+}$, it was observed that the fluorescence intensity decreased rapidly (Figure 3.11. (a)). By adding Cd and CN ions sequentially, switching cycles and reusability of the probe were demonstrated as shown in Figure 3.11. (b). Meantime studied with CN ions under the same conditions and quantities, it was seen that it gave the slightly different but evidentiary results with $CN^-$. The outcomes revealed that **BOD-MRY** has ON/OFF/ON sensor property.
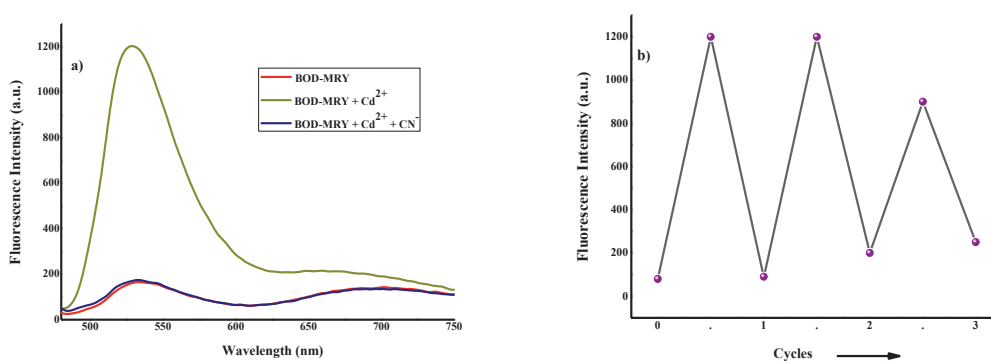


Figure 3.11. a) Emission spectra of reversibility study of **BOD-MRY** (20 µM) with $Cd^{2+}$ (1 eq.) and $CN^-$ (2 eq.) b) Fluorescence intensities of switching cycles of reversibility with the promotion of Cd and CN ions sequentially to **BOD-MRY** in ACN ($\lambda_{ex}$: 460 nm, $\lambda_{max}$: 525 nm)
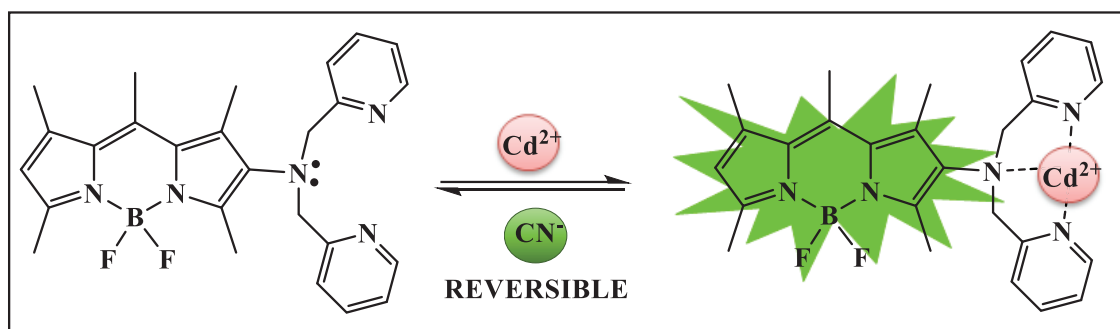
Figure 3.12. Proposed reversible binding of $Cd^{2+}$ to **BOD-MRY**

To enhance this study, metal scanning was carried out for anions additionally CN ions. As shown in Figure 3.13., there is no remarkable change in the fluorescence responses in the presence of anions interest.
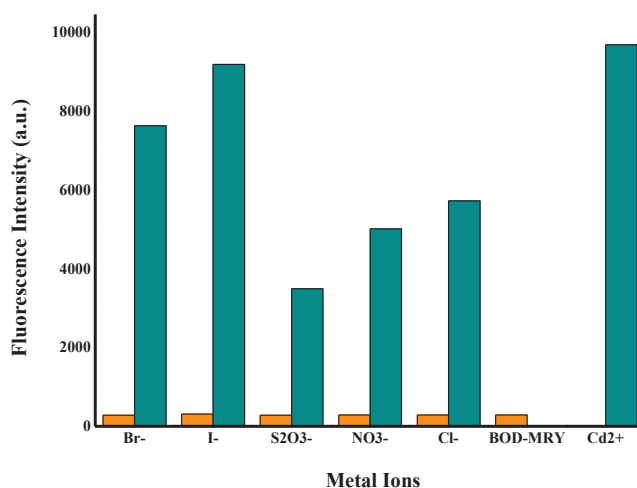


Figure 3.13. Fluorescence intensities of **BOD-MRY** (20 µM) only and **BOD-MRY** (20 µM) in 8:2 ACN/PBS at pH=7.0 at $\lambda_{max}$= 525 nm in the presence of 50.0 eq. of anions interest (orange columns) and fluorescence intensities of **BOD-MRY** (20 µM) in 8:2 ACN/PBS at pH=7.0 at $\lambda_{max}$=535 nm in the presence of $Cd^{2+}$ (50.0 eq.) and 50.0 eq. anions (cyan columns)

As the last investigation for the spectroscopic measurements, the binding process of $Cd^{2+}$ to **BOD-MRY** was observed by ^{1}H-NMR spectroscopy via the NMRS titration method (Fig. 3.14.). During $Cd^{2+}$ incubation which lasts approximately 5 minutes, observable changes in the ^{1}H-NMR spectra of **BOD-MRY** were distinguished. The peaks of all the protons affected by the coordination between cadmium ions and **BOD-MRY** ($H_a$, $H_c$, $H_e$, and $H_f$) shifted to a higher frequency. While the closer protons to the recognition site were observed at the

higher frequency in the spectra, relatively far ones from the nitrogens on the DPA ($H_b$ and $H_e$) had no significant shifts. Also, the non-symbol protons remained unchanged. Furthermore, a reorganization of the signals of the pyridyl and alkyl protons on the DPA unit confirmed the coordination between cadmium ions and the probe, **BOD-MRY**.
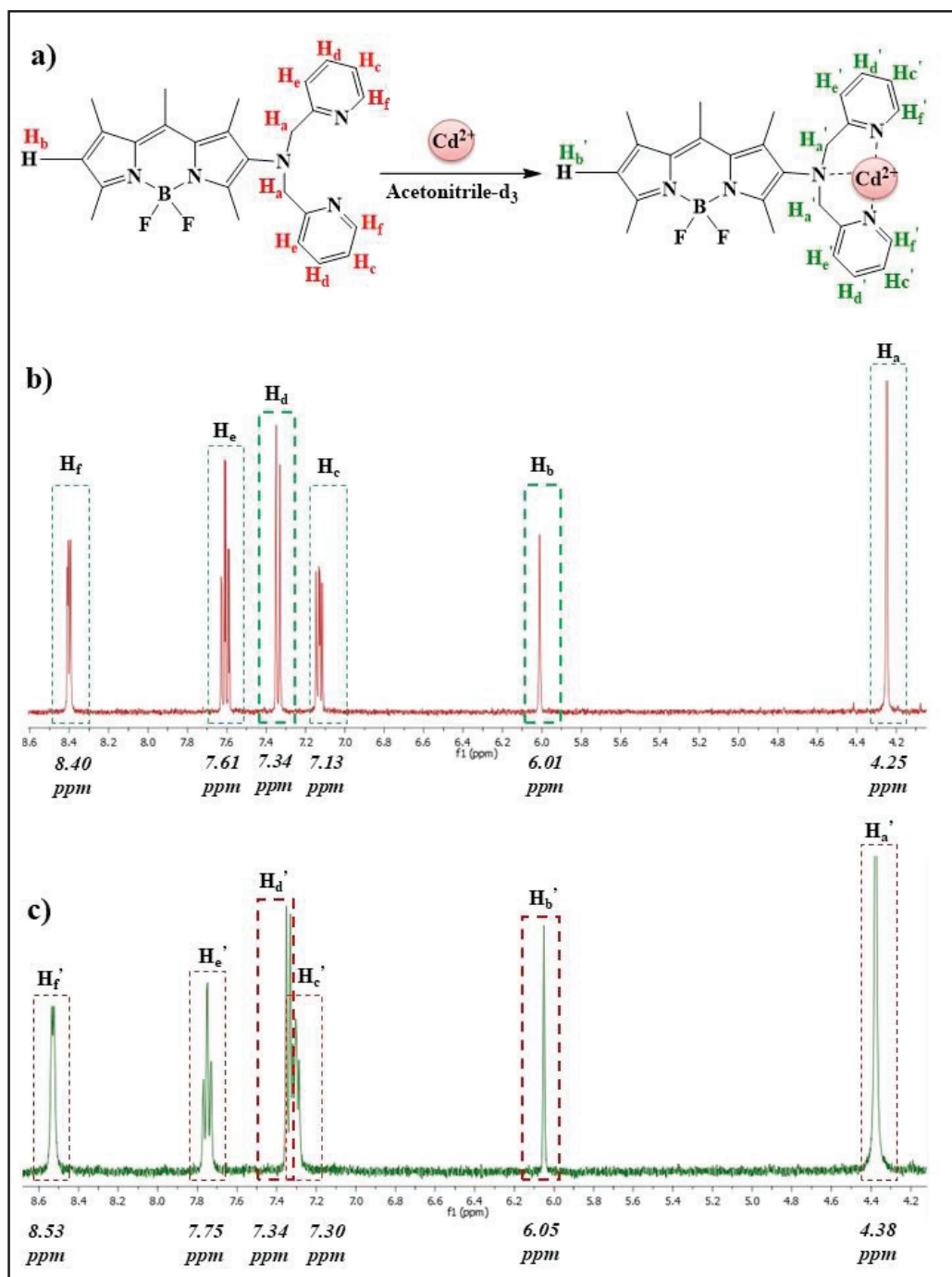


Figure 3.14. a) Proposed coordination mechanism of $Cd^{2+}$ to **BOD-MRY** b) $^1$H-NMR of **BOD-3** in ACN-d$_3$ c) $^1$H-NMR of **BOD-MRY** and $Cd^{2+}$ (1 eq.) in ACN-d$_3$

## 3.3. Cell Studies

The accomplished spectroscopic results of the probe were inciting to perform detection of the sensitivity of cadmium ions in cellular media using a fluorescence microscopy imaging system. The experiment was comprehensively executed according to the mentioned protocol in the previous chapter. Initially, A549 Human Lung Adenocarcinoma cells were treated 20 μM of **BOD-MRY**, 10 eq. of $Cd^{2+}$ and nucleus staining dye, DAPI (1.0 mM), respectively. After the treatment part, the cells were visualized by fluorescent microscopy. The fluorescent images of the fixed cell lines were taken before and after the addition of $Cd^{2+}$ separately. Weak fluorescence was observed in the cells in the absence of $Cd^{2+}$ ions. However, a substantial fluorescence emission enhancement was detected after the incubation of the cells with cadmium ions. Monitoring clearly of the turn-on response of the probe towards $Cd^{2+}$ in the cells demonstrated that the cells did not display any change in their morphology, and thus **BOD-MRY** was not toxic for the cells. The results also revealed that **BOD-MRY** is cell membrane penetrable could be used efficiently as a sensor for in vitro imaging of cadmium species in living cells (Figure 3.15.)



Figure 3.15. Fluorescence images of Human Lung Adenocarcinoma cells (A549) imaging of A549 cells treated with only **BOD-MRY** (20 μM) (first line) and with **BOD-MRY** (20 μM) and $Cd^{2+}$ (200 μM) ($\lambda_{ex}$=460 nm) (second line) a) Bright-field b) cells treated with DAPI c) cells untreated and treated with BOD-MRY, respectively d) merged images of frames a, b and c

# CHAPTER 4

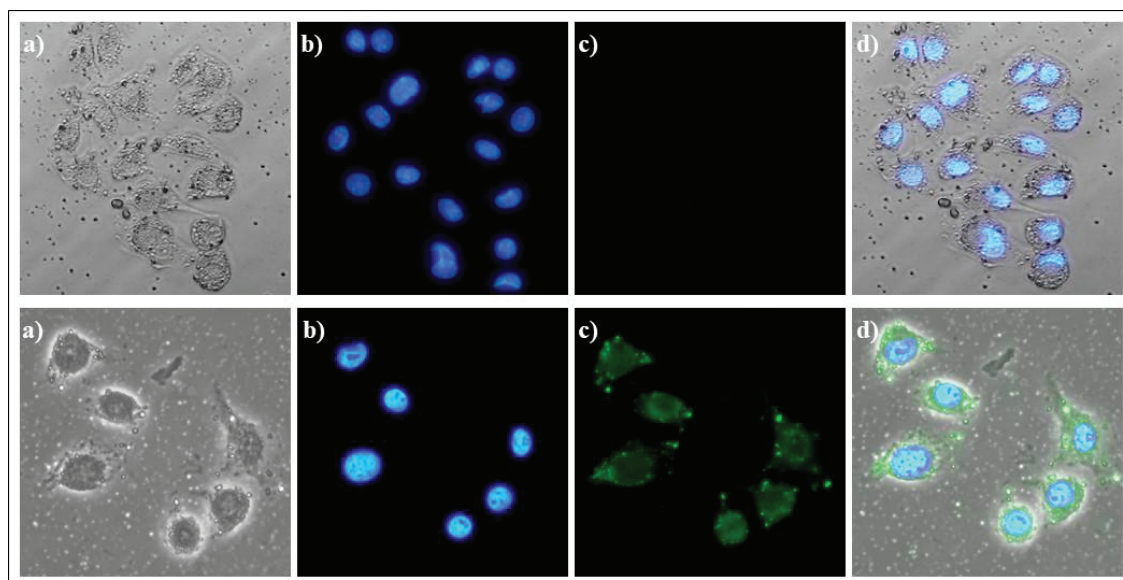# CONCLUSION

In conclusion, a new fluorescent probe that can differentiate Cd ions over other metal ions was designed and synthesized. Also, its spectroscopic characteristics and its permeability skills were investigated. BODIPY dye was used as a visible light-harvesting chromophore and derivatized with Di-(2-picolyl)amine (DPA) unit. DPA appears as a suitable binding platform for Cd ions. The probe, **BOD-MRY**, was quenched by the ICT mechanism which was removed in the existence of Cadmium ions due to the coordination of 3 nitrogens of the DPA unit with the metal ions.

The synthesis of **BOD-MRY** was confirmed by using NMR analysis and HRMS. Then, the photophysical properties of the probe were studied cautiously. The free **BOD-MRY** has faint fluorescence emission ($\Phi_F$= 0.0126) at 535 nm due to the ICT mechanism. After inhibition of the ICT by the coordination of the probe and metal ions, the probe produced a remarkable fluorescence emission enhancement ($\Phi_F$= 0.40) centered at 525 nm. The probe has a low detection limit of 279.5 nm in the ACN/PBS (8:2, v/v, pH=7.0) system and 2.2 nM in ACN. Additionally, the complex formed with a 1:1 stoichiometry ratio. **BOD-MRY** had no interference between the Cadmium ions and the other metal ions.

The cell-imaging capacity of the developed molecular sensor was also examined in human lung adenocarcinoma (A549) cells. No fluorescence was observed in the cells before the addition of Cadmium species; however, upon incubation with $Cd^{2+}$, the cells started to emit a fluorescence emission and it was concluded that **BOD-MRY** was able to pass through the cell membrane and detected $Cd^{2+}$ ions in cell lines.

# REFERENCES

Alnoman, R.; Stachelek, J.; Knight J. G.; Harriman, A.; Waddell, P. G. Synthesis of 2-aminoBODIPYs by palladium catalysed amination. *Org. Biomol. Chem.* **2017**, *15* (36), 7643-7653. https://doi.org/10.1039/C7OB01767G.

Arbeloa, F. L.; Ojeda, P. R.; Arbeloa, I. L. Fluorescence Self-Quenching of the Molecular Forms of Rhodamine B in Aqueous and Ethanolic Solutions. *J. Lumin.* **1989**, *44* (1–2), 105–112. https://doi.org/10.1016/0022-2313(89)90027-6.

Boens, N.; Verbelen, B.; Ortiz, M. J.; Jiao, L.; Dehaen, W. Synthesis of BODIPY Dyes through Postfunctionalization of the Boron Dipyrromethene Core. *Coord. Chem. Rev.* **2019**, *399*. https://doi.org/10.1016/j.ccr.2019.213024.

Callan, J. F.; De Silva, A. P.; Magri, D. C. Luminescent Sensors and Switches in the Early 21st Century. *Tetrahedron* **2005**, *61* (36), 8551–8588. https://doi.org/10.1016/j.tet.2005.05.043.

Cao, T.; Gong, D.; Zheng, L.; Wang, J.; Qian, J.; Liu, W.; Cao, Y.; Iqbal, K.; Qin, W.; Iqbal, A. BODIPY-Based Asymmetric Monosubstituted (Turn-on) and Symmetric Disubstituted (Ratiometric) Fluorescent Probes for Selective Detection of Phosgene in Solution and Gas Phase. *Anal. Chim. Acta.* **2019**, *1078*, 168–175.

Carter, K. P.; Young, A. M.; Palmer, A. E. Fluorescent Sensors for Measuring Metal Ions in Living Systems. *Chem. Rev.* **2014**, *114* (8), 4564–4601. https://doi.org/10.1021/cr400546e.

Cheng, D.; Liu, X.; Xie, Y.; Lv, H.; Wang, Z.; Yang, H.; Han, A.; Yang, X.; Zang, L. A Ratiometric Fluorescent Sensor for $Cd^{2+}$ Based on Internal Charge Transfer. *Sensors (Switzerland).* **2017**, *17* (11), 1–10. https://doi.org/10.3390/s17112517.

Duan, C.; Zhou, Y.; Shan, G. G.; Chen, Y.; Zhao, W.; Yuan, D.; Zeng, L.; Huang, X.; Niu, G. Bright Solid-State Red-Emissive BODIPYs: Facile Synthesis and Their High-Contrast Mechanochromic Properties. *J. Mater. Chem. C.* **2019**, *7* (12), 3471–3478. https://doi.org/10.1039/c8tc06421k.

Dukic-Cosic, D.; Baralic, K.; Javorac, D.; Djordjevic, A. B.; Bulat, Z. An Overview of Molecular Mechanisms in Cadmium Toxicity. *Current Opinion in Toxicology*. **2020**, *19*, 56–62. https://doi.org/10.1016/j.cotox.2019.12.002.

Guo, C.; Sedgwick, A. C.; Hirao, T.; Sessler, J. L. Supramolecular Fluorescent Sensors: An Historical Overview and Update. *Coord. Chem. Rev.* **2021**, *427*, 213560. https://doi.org/10.1016/j.ccr.2020.213560.

Gupta, M.; Parvathi, K.; Mula, S.; Maity, D. K.; Ray, A. K. Enhanced Fluorescence of Aqueous BODIPY by Interaction with Cavitand Cucurbit[7]Uril. *Photochem. Photobiol. Sci.* **2017**, *16* (4), 499–506. https://doi.org/10.1039/C6PP00325G.

Hatai, J.; Pal, S.; Jose, G. P.; Sengupta, T.; Bandyopadhyay, S. A Single-Molecule Multi Analyte Chemosensor Differentiates among Zn 2+, Pb 2+ and Hg 2+: Modulation of Selectivity by Tuning of Solvents. *RSC Adv.* **2012**, *2* (18), 7033–7036. https://doi.org/10.1039/c2ra20822a.

Kowada, T.; Maeda, H.; Kikuchi, K. BODIPY-Based Probes for the Fluorescence Imaging of Biomolecules in Living Cells. *Chem. Soc. Rev.* **2015**, *44* (14), 4953–4972. https://doi.org/10.1039/c5cs00030k.

Li, Y.; Chong, H.; Meng, X.; Wang, S.; Zhu, M.; Guo, Q. A Novel Quinoline-Based Two-Photon Fluorescent Probe for Detecting $Cd^{2+}$ in Vitro and in Vivo. *Dalt. Trans.* **2012**, *41* (20), 6189–6194. https://doi.org/10.1039/c2dt30192j.

Liu, W.; Xu, L.; Sheng, R.; Wang, P.; Li, H.; Wu, S. A Water-Soluble "Switching on" Fluorescent Chemosensor of Selectivity to $Cd^{2+}$. *Org. Lett.* **2007**, *9* (19), 3829–3832. https://doi.org/10.1021/ol701620h.

Liu, Z.; He, W.; Guo, Z. Metal Coordination in Photoluminescent Sensing. *Chem. Soc. Rev.* **2013**, *42* (4), 1568–1600. https://doi.org/10.1039/c2cs35363f.

Loudet, A.; Burgess, K. BODIPY Dyes and Their Derivatives: Syntheses and Spectroscopic Properties. *Chem. Rev*. **2007**, *107,* 4891–4932. https://doi.org/10.1021/cr078381n.

Maity, A.; Ghosh, U.; Giri, D.; Mukherjee, D.; Maiti, T. K.; Patra, S. K. A Water-Soluble BODIPY Based 'OFF/ON'' Fluorescent Probe for the Detection of $Cd^{2+}$ Ions with

High Selectivity and Sensitivity.' *Dalt. Trans.* **2019**, *48* (6), 2108–2117. https://doi.org/10.1039/c8dt04016h.

Monsma, F. J.; Barton, A. C.; Chol Kang, H.; Brassard, D. L.; Haugland, R. P.; Sibley, D. R. Characterization of Novel Fluorescent Ligands with High Affinity for D1 and D2 Dopaminergic Receptors. *J. Neurochem.* **1989**, *52* (5), 1641–1644. https://doi.org/10.1111/j.1471-4159.1989.tb09220.x.

Ni, Y.; Wu, J. Far-Red and near Infrared BODIPY Dyes: Synthesis and Applications for Fluorescent PH Probes and Bio-Imaging. *Org. Biomol. Chem.* **2014**, *12* (23), 3774–3791. https://doi.org/10.1039/c3ob42554a.

Ortiz, M. J.; Garcia-Moreno, I.; Agarrabeitia, A. R.; Duran-Sampedro, G.; Costela, A.; Sastre, R.; López Arbeloa, F.; Bañuelos Prieto, J.; López Arbeloa, I. Red-Edge-Wavelength Finely-Tunable Laser Action from New BODIPY Dyes. *Phys. Chem. Chem. Phys.* **2010**, *12* (28), 7804–7811. https://doi.org/10.1039/b925561c.

Pakalin, S.; Aschberger, K.; Cosgrove, O.; Coen, W. de; Paya-Perez, A.; Vegro, S. *European Union Summary Risk Assessment Report - Cadmium Metal and Cadmium Oxide*; Belgium, 2008.

Peng, X.; Du, J.; Fan, J.; Wang, J.; Wu, Y.; Zhao, J.; Sun, S.; Xu, T. A Selective Fluorescent Sensor for Imaging $Cd^{2+}$ in Living Cells. *J. Am. Chem. Soc.* **2007**, *129* (6), 1500–1501. https://doi.org/10.1021/ja0643319.

Piyanuch, P.; Patawanich, P.; Sirirak, J.; Suwatpipat, K.; Kamkaew, A.; Burgess, K.; Wanichacheva, N. Rapid and Visual Detection of $Cd^{2+}$ Based on Aza-BODIPY near Infrared Dye and Its Application in Real and Biological Samples for Environmental Contamination Screening. *J. Hazard. Mater.* **2021**, *409*, 124487. https://doi.org/10.1016/j.jhazmat.2020.124487.

Qin, W.; Dou, W.; Leen, V.; Dehaen, W.; Van Der Auweraer, M.; Boens, N. A Ratiometric, Fluorescent BODIPY-Based Probe for Transition and Heavy Metal Ions. *RSC Adv.* **2016**, *6* (10), 7806–7816. https://doi.org/10.1039/c5ra23751c.

Sahli, R.; Raouafi, N.; Boujlel, K.; Maisonhaute, E.; Schöllhorn, B.; Amatore, C. Electrochemically Active Phenylenediamine Probes for Transition Metal Cation

Detection. *New J. Chem.* **2011**, *35* (3), 709–715. https://doi.org/10.1039/c0nj00638f.

Sayar, M.; Karakuş, E.; Güner, T.; Yildiz, B.; Yildiz, U. H.; Emrullahoğlu, M. A BODIPY-Based Fluorescent Probe to Visually Detect Phosgene: Toward the Development of a Handheld Phosgene Detector. *Chem. - A Eur. J.* **2018**, *24* (13), 3136–3140. https://doi.org/10.1002/chem.201705613.

Tao, J.; Sun, D.; Sun, L.; Li, Z.; Fu, B.; Liu, J.; Zhang, L.; Wang, S.; Fang, Y.; Xu, H. Tuning the Photo-Physical Properties of BODIPY Dyes: Effects of 1, 3, 5, 7-Substitution on Their Optical and Electrochemical Behaviours. *Dye. Pigment.* **2019**, *168*, 166–174. https://doi.org/10.1016/j.dyepig.2019.04.054.

Teknikel, E.; Unaleroglu, C. Colorimetric and Fluorometric Ph Sensor Based on Bis(Methoxycarbonyl)Ethenyl Functionalized Bodipy. *Dye. Pigment.* **2015**, *120*, 239–244. https://doi.org/10.1016/j.dyepig.2015.04.021.

Tran, T. A.; Popova, L. P. Functions and Toxicity of Cadmium in Plants: Recent Advances and Future Prospects. *Turk. J. Botany* **2013**, *37* (1), 1–13. https://doi.org/10.3906/bot-1112-16.

Treibs, A.; Kreuzer, F. -H. Difluorboryl-Komplexe von Di- Und Tripyrrylmethenen. *Justus Liebigs Ann. Chem.* **1968**, *718* (1), 208–223. https://doi.org/10.1002/jlac.19687180119.

Turksoy, A.; Yildiz, D.; Akkaya, E. U. Photosensitization and Controlled Photosensitization with BODIPY Dyes. *Coord. Chem. Rev.* **2019**, *379*, 47–64. https://doi.org/10.1016/j.ccr.2017.09.029.

Xue, L.; Liu, C.; Jiang, H. Highly Sensitive and Selective Fluorescent Sensor for Distinguishing Cadmium from Zinc Ions in Aqueous Media. *Org. Lett.* **2009**, *11* (7), 1655–1658. https://doi.org/10.1021/ol900315r.

Zhang, H.; Reynolds, M. Cadmium Exposure in Living Organisms: A Short Review. *Science of the Total Environment.* **2019**, *678*, 761–767. https://doi.org/10.1016/j.scitotenv.2019.04.395.

# APPENDIX A

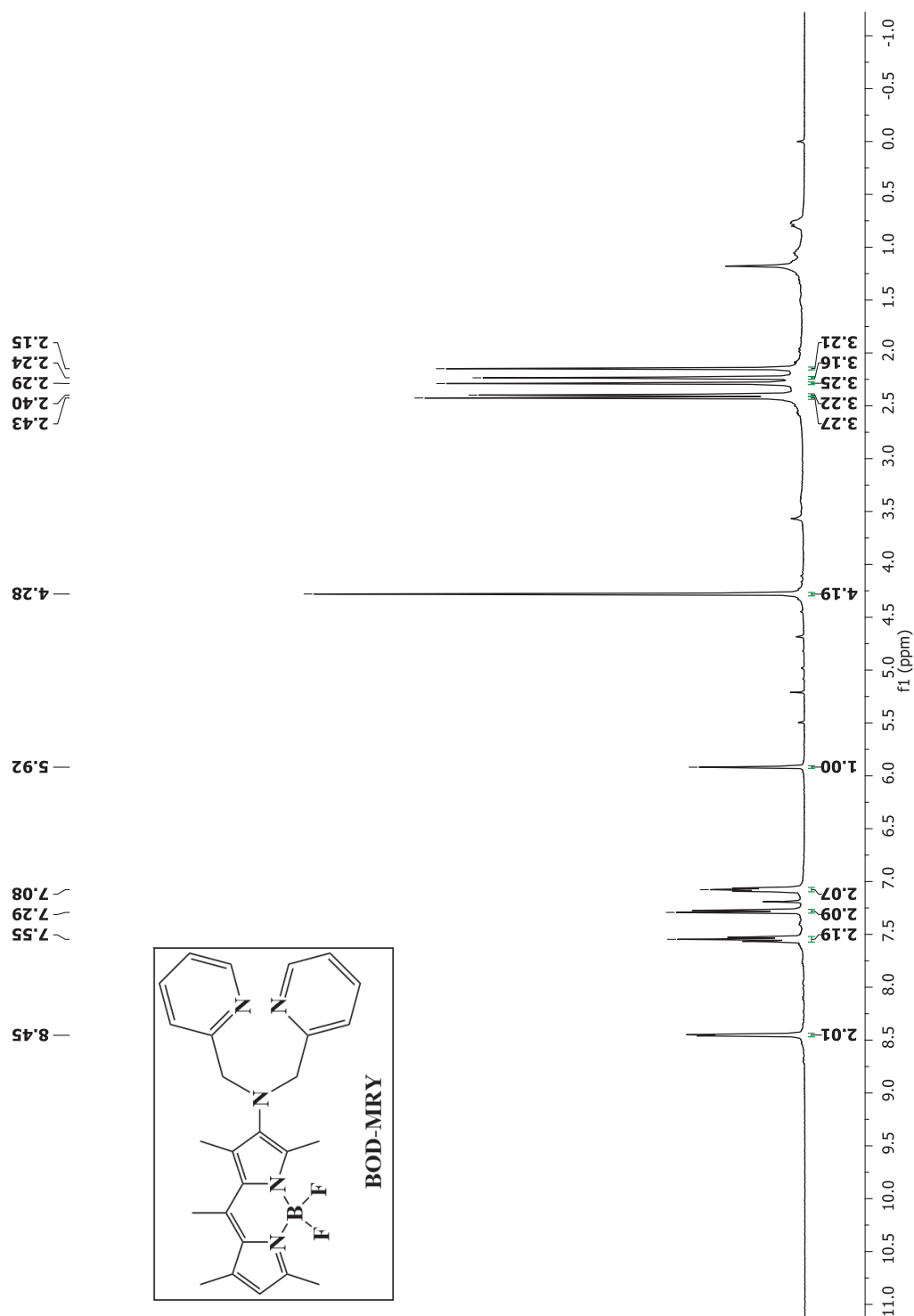## $^1$H-NMR AND $^{13}$C-NMR SPECTRA OF COMPOUNDS



Figure A.1. $^1$H NMR of 5,5-difluoro-1,3,7,9,10-pentamethyl-N,N-bis(pyridin-2-ylmethyl)-5H-5$\lambda^4$,6$\lambda^4$-dipyrrolo[1,2-c:2',1'-*f*][1,3,2]diazaborinin-2-amine
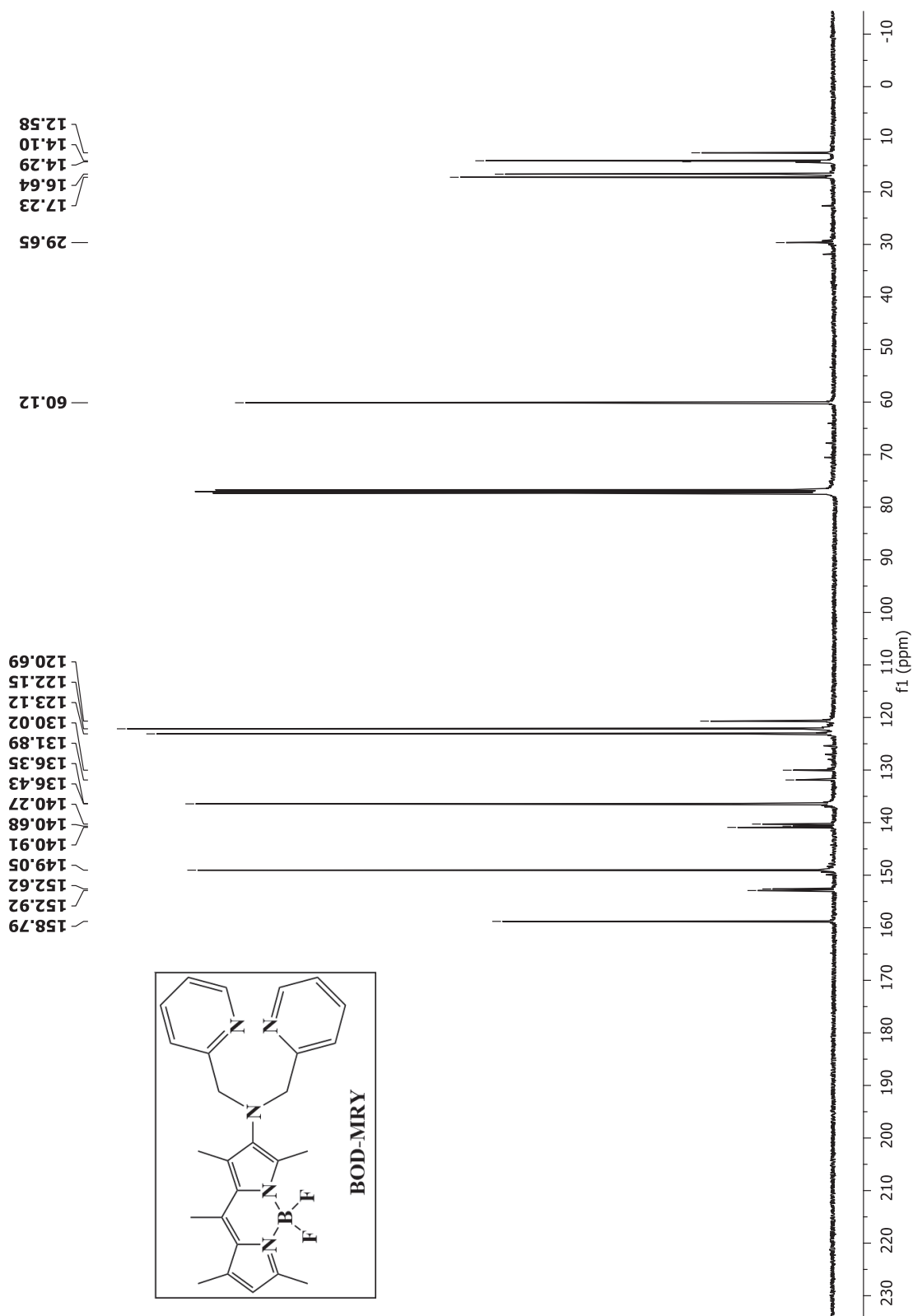
Figure A.2. $^{13}$C NMR of 5,5-difluoro-1,3,7,9,10-pentamethyl-N,N-bis(pyridin-2-ylmethyl)-5H-5$\lambda^4$,6$\lambda^4$-dipyrrolo[1,2-c:2',1'-*f*][1,3,2]diazaborinin-2-amine
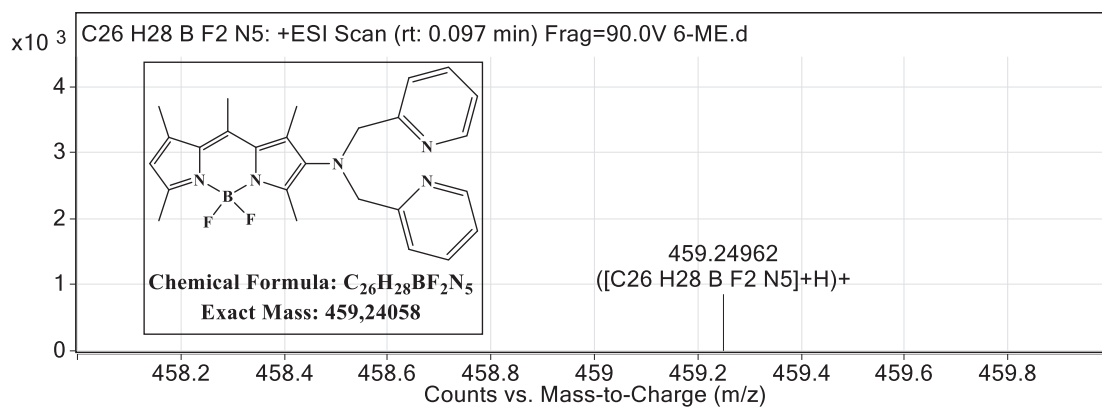
# APPENDIX B

# MASS SPECTRA OF COMPOUNDS



Figure B.1.  Mass spectrum of 5,5-difluoro-1,3,7,9,10-pentamethyl-N,N-bis(pyridin-2-ylmethyl)-5H-5$\lambda^4$,6$\lambda^4$-dipyrrolo[1,2-c:2',1'-*f*][1,3,2]diazaborinin-2-amine